
ON MCMC FOR VARIATIONALLY SPARSE GAUSSIAN PROCESSES: A PSEUDO-MARGINAL APPROACH

Karla Monterrubio-Gómez
MRC Human Genetics Unit
University of Edinburgh
kmonterr@ed.ac.uk

Sara Wade
School of Mathematics
University of Edinburgh
sara.wade@ed.ac.uk

ABSTRACT

Gaussian processes (GPs) are frequently used in machine learning and statistics to construct powerful models. However, when employing GPs in practice, important considerations must be made, regarding the high computational burden, approximation of the posterior, choice of the covariance function and inference of its hyperparameters. To address these issues, Hensman et al. [2015] combine variationally sparse GPs with Markov chain Monte Carlo (MCMC) to derive a scalable, flexible and general framework for GP models. Nevertheless, the resulting approach requires intractable likelihood evaluations for many observation models. To bypass this problem, we propose a pseudo-marginal (PM) scheme that offers asymptotically exact inference as well as computational gains through doubly stochastic estimators for the intractable likelihood and large datasets. In complex models, the advantages of the PM scheme are particularly evident, and we demonstrate this on a two-level GP regression model with a nonparametric covariance function to capture non-stationarity.

Keywords Gaussian process · variational inference · MCMC · pseudo-marginal · Poisson estimator

1 Introduction

Gaussian processes (GPs) are frequently used in machine learning and statistics to construct powerful models. In a Bayesian setting, GPs provide a probabilistic approach to model unknown functions; specifically, the GP prior assumes that the function evaluated at any finite set of inputs has a Gaussian distribution with consistent parameters, specified by the mean function and symmetric positive definite covariance (or kernel) function. The flexible, probabilistic and nonparametric nature of GP models makes them appropriate and useful in a wide range of applications, including geostatistics [Matheron, 1973], atmospheric sciences [Berrocal et al., 2010], biology [Stathopoulos et al., 2014], inverse problems [Kaipio and Somersalo, 2006], and more. However, when employing GPs in practice, important considerations must be made, specifically, to address the computational burden, approximation of the posterior, form of the covariance function and inference of its hyperparameters.

First, GPs suffer from a high computational burden, due to the need to store and invert large and dense covariance matrices. To overcome this, various schemes have been proposed, including local approximations [Rasmussen and Ghahramani, 2002, Tresp, 2000], predictive processes [Banerjee et al., 2008], basis function approximations [Cressie and Johannesson, 2008], sparse formulations of the precision matrix [Lindgren et al., 2011, Grigorievskiy et al., 2017, Durrande et al., 2019], and others (see Heaton et al. [2019] and Rasmussen and Williams [2006, Chap. 8] for reviews of approaches in spatial statistics and machine learning, respectively). In machine learning, the sparse GP approximation based on a set of inducing points or pseudo inputs is one of the most popular approaches, due to its general applicability, with no requirements or assumptions on the data structure or covariance function. Early work in this direction includes Seeger et al. [2003] and Snelson and Ghahramani [2006], and in this paper, we focus on the variational inducing point framework introduced in Titsias [2009].

Second, while GP priors result in tractable posterior inference in a normal regression setting, many statistical and machine learning tasks require other likelihoods, necessitating approximation of the posterior. Markov chain Monte Carlo (MCMC) provides a general way to simulate from the posterior and is often considered a gold standard in

Bayesian inference, due to its asymptotic guarantees. However, the computational complexity and high-dimensionality of GP models prohibits the use of MCMC algorithms for large datasets. Variational methods are a popular alternative to MCMC schemes and commonly employed in machine learning for faster, approximate inference [Blei et al., 2017]. More specifically, for GP models, variational inference is an active area of research [e.g. Titsias, 2009, Matthews et al., 2016, Hensman et al., 2013, Cutajar et al., 2019, Damianou and Lawrence, 2013], but models are typically restricted to a fixed family of likelihoods.

Lastly, the form of the covariance function and its hyperparameters crucially determine properties of the unknown function, such as the spatial correlation, smoothness, and periodicity. Typically, parametric forms are specified for the covariance function, and the hyperparameters are inferred via a hierarchical or an empirical Bayes approach, which is critical to allow the model to adapt to the true smoothness of the function and achieve desirable posterior consistency and coverage [Sniekers and van der Vaart, 2015]. In a hierarchical approach, MCMC algorithms have been proposed [Yu and Meng, 2011, Filippone and Girolami, 2014b] but require costly operations on large, dense covariance matrices at every iteration. Variational schemes employ (approximate) empirical Bayes, or maximum marginal likelihood estimation, and while such operations are still required, the number of iterations is typically much reduced. Furthermore, the parametric assumption of the covariance function limits the model’s ability to recover changing behavior of the function, e.g. different smoothness levels, across the input space. Thus, more complex model structures have been proposed to combine multiple GPs for increased model flexibility [Dunlop et al., 2018, Gadd et al., 2020], which pose further challenges for inference.

To address these issues, we build on the work of Hensman et al. [2015], which combines the variational inducing point framework of Titsias [2009] with MCMC to derive a scalable yet flexible and general framework for GP models. Their sparse variational method results in a low-dimensional approximate posterior, where MCMC is employed to draw samples. Thus, the variationally sparse MCMC framework benefits from (i) the sparse variational method to alleviate the computational burden, (ii) a general scheme for any factorized likelihood, and (iii) full posterior inference of the hyperparameters. The flexibility, generality and theoretical guarantees of MCMC allow them to apply the framework to general tasks, removing restrictions on the likelihood, and importantly, avoid any further distributional assumptions on the low-dimensional posterior, e.g. independence, that are typically required in full variational schemes.

Nevertheless, the resulting optimal approximate posterior requires exponentiated expected log-likelihood evaluations that are intractable for many observation models, including classification problems, robust GP regression with the student t likelihood, stochastic volatility models, and various others [Nickisch and Rasmussen, 2008, Hernández-Lobato et al., 2011, Neal, 1997, Wu et al., 2014]. In this case, Hensman et al. [2015] suggest approximating the required expectations with Gauss-Hermite quadrature. This clearly introduces an additional level of approximation, which can have adverse effects on the accuracy and computational cost of the method. In complex models, such effects may be particularly severe, and we demonstrate this on the two-level GP regression model with a nonparametric covariance function to capture non-stationarity [Monterrubio-Gómez et al., 2020].

We propose an alternative approach to bypass this problem by replacing the intractable likelihood evaluation with a computationally cheap unbiased estimate based on the block-Poisson estimator introduced by Quiroz et al. [2020]. Our proposed framework offers asymptotically exact inference for the low-dimensional variational posterior through a pseudo-marginal scheme as well as computational gains through doubly stochastic estimators for the intractable likelihood evaluations and large datasets.

This paper is organised as follows. We start, in Section 2, with a review of variationally sparse GP models, where we focus on the work of Hensman et al. [2015]. Section 3 introduces the signed block-Poisson pseudo-marginal (S-BP-PM) scheme for variationally sparse GPs. Section 4 showcases the limitations of the Gauss-Hermite quadrature approximation employing, as an example, a non-stationary 2-level GP model as well as details of the S-BP-PM scheme for this model. Later, Section 5 demonstrates our proposed scheme on a 1-dimensional 2-level GP regression model. Finally, Section 6 concludes summarising the main findings.

2 Variationally sparse GPs

The observed data are assumed to consist of outputs y_n , which may be real-valued or more generally binary, counts, etc., with corresponding input locations $\mathbf{x}_n \in \mathbb{R}^D$ for $n = 1, \dots, N$. The likelihood is assumed to factorise across data points, dependent on an latent function $z : \mathbb{R}^D \rightarrow \mathbb{R}$ that maps the input locations to the real line:

$$p(\mathbf{y} \mid \mathbf{z}, \boldsymbol{\rho}) = \prod_{n=1}^N p(y_n \mid z(\mathbf{x}_n), \boldsymbol{\rho}),$$

where $\mathbf{y} = (y_1, \dots, y_N)^T$, $\mathbf{z} = (z_1, \dots, z_N)^T$ with $z_n \equiv z(\mathbf{x}_n)$, and $\boldsymbol{\rho}$ contains any additional likelihood parameters. The unknown function z has a Gaussian process prior with zero mean and covariance function $C_\phi(\cdot, \cdot)$ parametrised by ϕ , namely, $z(\cdot) \sim \text{GP}(0, C_\phi(\cdot, \cdot))$.

To overcome the computational complexity of GPs, Snelson and Ghahramani [2006] proposed the sparse pseudo-input framework. The key idea of this approach is to augment the data with a set of $M \ll N$ inducing or pseudo-points $\tilde{\mathbf{X}} = (\tilde{\mathbf{x}}_1, \dots, \tilde{\mathbf{x}}_M)^T$ and collect the values of the latent functions at the inducing points into the vectors $\tilde{\mathbf{z}} = (\tilde{z}_1, \dots, \tilde{z}_M)^T$, where $\tilde{z}_m \equiv z(\tilde{\mathbf{x}}_m)$, and we refer to the \tilde{z}_m as the *inducing variables*. By properties of GPs, the augmented prior is

$$\begin{aligned} \pi(\mathbf{z}, \tilde{\mathbf{z}} \mid \phi) &= \pi(\mathbf{z} \mid \tilde{\mathbf{z}}, \phi) \pi(\tilde{\mathbf{z}} \mid \phi) \\ &= \text{N}\left(\mathbf{z} \mid \mathbf{C}_{\mathbf{z}, \tilde{\mathbf{z}}} \mathbf{C}_{\tilde{\mathbf{z}}, \tilde{\mathbf{z}}}^{-1} \tilde{\mathbf{z}}, \mathbf{C}_{\mathbf{z}, \mathbf{z}} - \mathbf{C}_{\mathbf{z}, \tilde{\mathbf{z}}} \mathbf{C}_{\tilde{\mathbf{z}}, \tilde{\mathbf{z}}}^{-1} \mathbf{C}_{\tilde{\mathbf{z}}, \mathbf{z}}\right) \text{N}(\tilde{\mathbf{z}} \mid 0, \mathbf{C}_{\tilde{\mathbf{z}}, \tilde{\mathbf{z}}}), \end{aligned}$$

where we make use of the short notation $\mathbf{C}_{\mathbf{z}, \mathbf{z}}$ and $\mathbf{C}_{\tilde{\mathbf{z}}, \tilde{\mathbf{z}}}$ to denote the covariance matrix constructed by evaluating the kernel at the inputs \mathbf{X} and $\tilde{\mathbf{X}}$, respectively, and $\mathbf{C}_{\mathbf{z}, \tilde{\mathbf{z}}}$ to denote the cross-covariance matrix between the the function evaluated at the inputs \mathbf{X} and inducing points $\tilde{\mathbf{X}}$. Under the augmented model, the posterior of the parameters and latent variables is given by:

$$\pi(\mathbf{z}, \tilde{\mathbf{z}}, \boldsymbol{\rho}, \phi \mid \mathbf{y}, \mathbf{X}) \propto \prod_{n=1}^N p(y_n \mid z_n, \boldsymbol{\rho}) \pi(\mathbf{z} \mid \tilde{\mathbf{z}}, \phi) \pi(\tilde{\mathbf{z}} \mid \phi) \pi(\phi) \pi(\boldsymbol{\rho}).$$

The variationally sparse approach of Hensman et al. [2015] restricts the approximate variational posterior to take the form:

$$q(\mathbf{z}, \tilde{\mathbf{z}}, \boldsymbol{\rho}, \phi) \propto \pi(\mathbf{z} \mid \tilde{\mathbf{z}}, \phi) q(\tilde{\mathbf{z}}, \boldsymbol{\rho}, \phi). \quad (1)$$

Note that in the right-hand side of Eq. (1), the first term corresponds to the prior predictive distribution of \mathbf{z} given $\tilde{\mathbf{z}}$, while the second is the joint approximate posterior of the inducing variables, parameters, and hyperparameters. Thus, the variationally sparse approach assumes that conditioned on the inducing variables and hyperparameters, the latent function at the observed input locations does not depend on the data. This assumption is crucial to achieve the desired scalability, but the accuracy of this approximation clearly depends on the number and locations of the inducing points. Under this assumption, Hensman et al. [2015] showed that the optimal low-dimensional variational posterior (the second term in Eq. (1)), which is obtained by minimizing the Kullback-Leibler (KL) divergence between the approximate and true posterior, $\text{KL}(q(\mathbf{z}, \tilde{\mathbf{z}}, \boldsymbol{\rho}, \phi) \parallel \pi(\mathbf{z}, \tilde{\mathbf{z}}, \boldsymbol{\rho}, \phi \mid \mathbf{y}, \mathbf{X}))$, takes the form

$$q(\tilde{\mathbf{z}}, \boldsymbol{\rho}, \phi) \propto \exp\left(\sum_{n=1}^N \mathbb{E}_{\pi(\mathbf{z}_n \mid \tilde{\mathbf{z}}, \phi)} [\log(p(y_n \mid z_n, \boldsymbol{\rho}))]\right) \pi(\tilde{\mathbf{z}} \mid \phi) \pi(\phi) \pi(\boldsymbol{\rho}). \quad (2)$$

Computation of Eq. (2) involves expectations over univariate Gaussian random variables, which are available analytically only for certain tasks, specifically, for Gaussian or Poisson likelihoods. In all other settings, Hensman et al. [2015] suggest to approximate with Gauss-Hermite quadrature. In addition, to avoid placing any further restrictions on the form of the optimal variational posterior, Hensman et al. [2015] propose to use MCMC methods to sample from a whitened version of Eq. (2). Whitening is employed because Eq. (2) exhibits high correlations between $\tilde{\mathbf{z}}$ and ϕ , which can result in poor mixing. Thus, the target distribution is:

$$q(\tilde{\boldsymbol{\xi}}, \boldsymbol{\rho}, \phi) \propto \exp\left(\sum_{n=1}^N \mathbb{E}_{\pi(\mathbf{z}_n \mid \tilde{\boldsymbol{\xi}}, \phi)} [\log(p(y_n \mid z_n, \boldsymbol{\rho}))]\right) \text{N}(\tilde{\boldsymbol{\xi}} \mid 0, \mathbf{I}_M) \pi(\phi) \pi(\boldsymbol{\rho}), \quad (3)$$

with $\tilde{\mathbf{z}} = \mathbf{L}(\phi) \tilde{\boldsymbol{\xi}}$, where $\tilde{\boldsymbol{\xi}} \sim \text{N}(0, \mathbf{I}_M)$ and $\mathbf{L}(\phi) \mathbf{L}(\phi)^T = \mathbf{C}_{\tilde{\mathbf{z}}, \tilde{\mathbf{z}}}$.

While this results in a scalable and flexible approach for general GP-based models, the Gauss-Hermite quadrature clearly introduces an extra level of approximation, which can adversely affect the accuracy and cost. The error of the quadrature approximation has been carefully studied in literature [Gautschi, 1981, Mastroianni and Monegato, 1994, Arasaratnam et al., 2007], and in general, Gauss-Hermite quadrature of order J provides a good approximation if the integrand, denoted by $g(\cdot)$, is a polynomial of order $2J - 1$ or less. When this is not the case, the error of the approximation corresponds to $J! g^{(2J)}(\epsilon) / 2J!$, where $g^{(2J)}(\cdot)$ is the $2J$ -th derivative of $g(\cdot)$. In simple settings, such as binary classification, the computational complexity for a likelihood evaluation is $\mathcal{O}(NM^2 + NJ)$ and sufficient approximation may be achieved with relatively small J . However, the computational cost can increase drastically for more complex models, e.g. $\mathcal{O}(JNM^2)$ in the two-level GP model of Section 4, which also requires a large J for good approximation. Moreover, for some tasks, such as multinomial classification, multivariate quadrature is needed, which further exacerbates costs and accuracy issues.

When quadrature approximation is required, the scheme of Hensman et al. [2015] belongs to the class of approximate MCMC methods [Marjoram et al., 2003]. Recently, Vihola et al. [2020] proposed an importance sampling correction of approximate MCMC to yield exact inference. While this could be applied to the scheme of Hensman et al. [2015], instead, in the next section, we construct a pseudo-marginal sampler based on the block-Poisson estimator of Quiroz et al. [2020]. Importantly, our scheme bypasses the problems of the approximate MCMC scheme, by providing both asymptotically exact inference for the optimal variational posterior and reduced computational complexity.

3 PM for variationally sparse GPs

The pseudo-marginal (PM) approach introduced by Beaumont [2003] and Andrieu et al. [2009] provides a route to do exact Bayesian inference in models with intractable or expensive likelihoods. PM samplers employ a non-negative unbiased estimator of the likelihood in place of the intractable or expensive function in a Metropolis-Hasting (MH) algorithm to produce asymptotically exact samples from the posterior distribution. In particular, PM schemes have been previously employed to do inference in GP models [see, e.g. Filippone and Girolami, 2014a, Murray and Graham, 2016, Xiong et al., 2017].

The key ingredient of PM schemes is the unbiased estimator of the likelihood, and as such, different approaches exist to produce the unbiased estimator in different scenarios. For expensive likelihoods due to tall data, subsampling-based strategies include the Rhee-Glynn estimator [Rhee and Glynn, 2015, Bardenet et al., 2017] or PM Firefly [MacLaurin and Adams, 2015, Bardenet et al., 2017]. For intractable likelihoods, unbiased estimators have been proposed using, for example, importance sampling [Filippone and Girolami, 2014a], annealed importance sampling [Filippone, 2014], particle filters [Andrieu et al., 2010], and generalized Poisson estimation [Fearnhead et al., 2008]. However, the variance of estimator needs to be carefully controlled; if too high, the likelihood may be overestimated, making it difficult for the chain to leave the current state. Indeed, Doucet et al. [2015] recommend keeping the variance of the log-likelihood estimator to 1.5, in order to balance computation time with low variance of the MCMC estimates.

Recently, Quiroz et al. [2020] proposed combining an importance sampling sign correction [Lyne et al., 2015] with a product of Poisson estimators [Fearnhead et al., 2010] to derive a signed block-Poisson pseudo-marginal scheme for fast, exact inference in tall datasets. Their block-Poisson estimator is appealing for several reasons. First, through the product form, correlation is introduced between the log estimated likelihood at current and proposed states, resulting in an efficient dependent PM scheme [Deligiannidis et al., 2018], that can accommodate noisier likelihood estimates. In addition, it has lower variance than the Rhee-Glynn estimator [Rhee and Glynn, 2015, Bardenet et al., 2017] and makes use of control variates for variance reduction. Lastly, a sign correction permits employing a soft-lower bound (as opposed to the strict lower bound in Bardenet et al. [2017]), which is more computationally efficient.

In this work, we build on Quiroz et al. [2020] to construct a signed block-Poisson PM scheme for variationally sparse GPs, that is both computationally efficient for large datasets and offers asymptotically exact inference for the low-dimensional variational posterior. This is accomplished through a variant of the PM scheme that employs a doubly stochastic estimator for the intractable exponentiated expected log-likelihood, by also data subsampling.

3.1 Doubly stochastic block-Poisson estimator

Our goal is find an unbiased estimator, \hat{E} , of the intractable exponentiated expected log-likelihood term in Eq. (3):

$$E = \exp \left(\sum_{n=1}^N \mathbb{E}_{\pi(z_n | \xi, \phi)} [\log(p(y_n | z_n, \rho))] \right),$$

that is also computationally efficient for large sample sizes. To do so, we follow Quiroz et al. [2020] by employing subsampling for computational efficiency and control variates to reduce the variance of our estimator. In addition, we employ a further layer of stochasticity in our estimator to deal with the intractable expectation.

Using the simplifying notation $l(y_n | z_n, \rho) = \log(p(y_n | z_n, \rho))$, the first step in this direction is to define the difference $d = \sum_{n=1}^N d_n$, with

$$d_n = \mathbb{E}_{\pi(z_n | \xi, \phi)} [l(y_n | z_n, \rho)] - \bar{\nu}_n, \quad (4)$$

where the control variate $\bar{\nu}_n$ is an approximation to $\mathbb{E}_{\pi(z_n | \xi, \phi)} [l(y_n | z_n, \rho)]$. Thus, we have

$$\log(E) = d + \sum_{n=1}^N \bar{\nu}_n.$$

Specifically, assuming differentiability of $l(y \mid z, \boldsymbol{\rho})$ with respect to z , we define $\bar{\nu}_n$ through a first-order Taylor-expansion around $\mathbb{E}[z_n]$ (with the expectation taken with respect to $\pi(z_n \mid \tilde{\boldsymbol{\xi}}, \phi)$):

$$\nu_n(z_n) = l(y_n \mid \mathbb{E}[z_n], \boldsymbol{\rho}) + (z_n - \mathbb{E}[z_n])l'(y_n \mid \mathbb{E}[z_n], \boldsymbol{\rho}), \quad (5)$$

such that

$$\bar{\nu}_n = \mathbb{E}_{\pi(z_n \mid \tilde{\boldsymbol{\xi}}, \phi)}[\nu_n(z_n)] = l(y_n \mid \mathbb{E}[z_n], \boldsymbol{\rho}). \quad (6)$$

We note that more generally, a multivariate Taylor expansion may be used in models involving multiple Gaussian processes.

By defining $\nu_n(z_n)$ through Eq. (5), the difference in Eq. (4) can be equivalently written as

$$d_n = \mathbb{E}_{\pi(z_n \mid \tilde{\boldsymbol{\xi}}, \phi)}[l(y_n \mid z_n, \boldsymbol{\rho}) - \nu_n(z_n)],$$

and an unbiased difference estimator for d_n is

$$\hat{d}_n = l(y_n \mid z_n, \boldsymbol{\rho}) - \nu_n(z_n), \quad (7)$$

with $z_n \sim \pi(z_n \mid \tilde{\boldsymbol{\xi}}, \phi)$. We then use subsampling techniques to obtain

$$\hat{d}_B = \frac{N}{B} \sum_{b=1}^B \hat{d}_{\alpha_b}, \quad (8)$$

where $\alpha_b \stackrel{\text{iid}}{\sim} \text{Unif}(1, \dots, N)$ indexes a subsample of size B that is taken with replacement. The variance of the estimator in Eq. (8) is $\mathbb{V}[\hat{d}_B] = \gamma/B$ with $\gamma = N^2 \mathbb{V}[\hat{d}_{\alpha_b}]$ denoting the intrinsic variance of the estimator.

Thus, $\hat{d}_B + \sum_{n=1}^N \bar{\nu}_n$ provides an unbiased estimator of the expected log-likelihood. Clearly, simply exponentiating this does not provide an unbiased estimator of E , and in order to do so, we employ block-Poisson estimation [Quiroz et al., 2020]. In the doubly stochastic block-Poisson estimator in Definition 1, we re-write the difference estimator in Eq. (7) in terms of random variables that do not depend on $(\tilde{\boldsymbol{\xi}}, \phi)$. Thus, we introduce uniform random variables, χ_1, \dots, χ_N , and apply the inverse CDF transformation to produce samples z_n needed to evaluate Eq. (7).

Definition 1. *The doubly stochastic block-Poisson estimator is*

$$\hat{E} = \exp \left(\sum_{n=1}^N l(y_n \mid \mathbb{E}[z_n], \boldsymbol{\rho}) \right) \prod_{k=1}^{\kappa} \exp \left(\frac{a + \kappa}{\kappa} \right) \prod_{h=1}^{\mathcal{H}_k} \left(\frac{\hat{d}_B^{h,k} - a}{\kappa} \right) \quad (9)$$

with $\kappa \in \mathbb{Z}^+$, $\mathcal{H}_1, \dots, \mathcal{H}_\kappa \sim \text{Pois}(1)$, $a \in \mathbb{R}$ a lower bound for

$$\hat{d}_B^{h,k} = \frac{N}{B} \sum_{b=1}^B \hat{d}_{\alpha_b^{h,k}}, \text{ with } \hat{d}_{\alpha_b^{h,k}} = l(y_{\alpha_b^{h,k}} \mid z_{\alpha_b^{h,k}}, \boldsymbol{\rho}) - \nu_{\alpha_b^{h,k}}(z_{\alpha_b^{h,k}}),$$

where $\alpha_b^{h,k}$ is uniformly sampled from $(1, \dots, N)$; $\chi_b^{h,k} \sim \text{Unif}(0, 1)$, and the log-likelihood and Taylor expansion in $\hat{d}_{\alpha_b^{h,k}}$ are evaluated with $z_{\alpha_b^{h,k}} = F_{z_{\alpha_b^{h,k}}}^{-1}(\chi_b^{h,k})$, where $F_{z_n}^{-1}$ denotes the inverse CDF of Gaussian prior predictive of z_n given $(\tilde{\boldsymbol{\xi}}, \phi)$.

Evaluation of the likelihood estimator in Eq. (9) requires computation of both the control variates across every data point and, on average, κ difference estimators. Note that the control variates only depend on the predictive means $\mathbb{E}[z_n \mid \tilde{\boldsymbol{z}}] = \mathbf{C}_{z_n, \tilde{\boldsymbol{z}}} \mathbf{C}_{\tilde{\boldsymbol{z}}, \tilde{\boldsymbol{z}}}^{-1} \tilde{\boldsymbol{z}}$, with complexity $\mathcal{O}(NM + M^3)$. The difference estimator, instead, requires also the predictive variance $\mathbb{V}(z_n \mid \tilde{\boldsymbol{z}}) = \mathbf{C}_{z_n, z_n} - \mathbf{C}_{z_n, \tilde{\boldsymbol{z}}} \mathbf{C}_{\tilde{\boldsymbol{z}}, \tilde{\boldsymbol{z}}}^{-1} \mathbf{C}_{\tilde{\boldsymbol{z}}, z_n}$, but only across all subsets, with complexity $\mathcal{O}(\kappa BM^2 + M^3)$. Thus, evaluation of the block-Poisson estimator is $\mathcal{O}(NM + \kappa BM^2 + M^3)$, in contrast to the $\mathcal{O}(NM^2 + M^3)$ required by the approximate scheme of Hensman et al. [2015].

We highlight that Quiroz et al. [2020] focus on tall data with tractable likelihoods, and thus, provide an alternate construction of the difference estimator, considering two types of control variates, parameter expanded and data expanded, that reduce the computational complexity to a small number of evaluations that does not depend on N . Quiroz et al. [2019] examine properties of such control variates in balancing computation time with variance reduction. Variants of these control variates could be developed here to further reduce the computational complexity and remove dependency on N ; however, we do not pursue this, in order to maintain low variance of the doubly stochastic estimator.

Algorithm 1 Signed block-Poisson pseudo-marginal sampler (S-BP-PM)

Require: Target distribution: $\tilde{q}(\tilde{\xi}, \phi, \rho)$, initial states: $\tilde{\xi}^{(0)}, \phi^{(0)}, \rho^{(0)}$, iterations: T , number of Poisson estimators: κ , batch size: B ; lower bound: a , initial means: c_1, \dots, c_n , initial random variates $(\mathcal{V}_1, \dots, \mathcal{V}_G)$, initial estimator \hat{E} .

```

1: for  $t = 1, \dots, T$  do
2:   Draw  $\rho^*$  from  $q(\rho | \rho^{(t-1)})$ 
3:   Compute control variates:  $l_n = l(y_n | c_n, \rho^*)$  for  $n = 1, \dots, N$ 
4:   Sample a block  $g$  and random variates  $\mathcal{V}_g^*$ .
5:   Compute  $\log(|\hat{E}^*|)$  using Eq. (9)
6:   Set  $\rho^{(t)} \leftarrow \rho^*$ ;  $\mathcal{V}_g \leftarrow \mathcal{V}_g^*$ ;  $\log(|\hat{E}|) \leftarrow \log(|\hat{E}^*|)$ ; and  $\mathcal{S}_\rho^{(t)} \leftarrow \text{sign}(\hat{E}^*)$  with
7:     probability:  $\min \left\{ 1, \frac{|\hat{E}^*| \pi(\rho^*) q(\rho^{(t-1)} | \rho^*)}{|\hat{E}| \pi(\rho^{(t-1)}) q(\rho^* | \rho^{(t-1)})} \right\}$ 
8:   Else  $\rho^{(t)} \leftarrow \rho^{(t-1)}$  and  $\mathcal{S}_\rho^{(t)} \leftarrow \mathcal{S}_\rho^{(t-1)}$ 
9:   Draw  $\tilde{\xi}^*$  from  $q(\tilde{\xi} | \tilde{\xi}^{(t-1)})$ 
10:  Compute GP predictive means  $c_n^*$  and control variates:  $l_n = l(y_n | c_n^*, \rho^{(t)})$ 
11:    for  $n = 1, \dots, N$ 
12:  Sample a block  $g$  and random variates  $\mathcal{V}_g^*$ .
13:  Compute  $\log(|\hat{E}^*|)$  using Eq. (9)
14:  Set  $\tilde{\xi}^{(t)} \leftarrow \tilde{\xi}^*$ ;  $\mathcal{V}_g \leftarrow \mathcal{V}_g^*$ ;  $\log(|\hat{E}|) \leftarrow \log(|\hat{E}^*|)$ ;  $\mathcal{S}_\xi^{(t)} \leftarrow \text{sign}(\hat{E}^*)$ ; and
15:     $c_{1:N} \leftarrow c_{1:N}^*$  with probability:  $\min \left\{ 1, \frac{|\hat{E}^*| \pi(\tilde{\xi}^*) q(\tilde{\xi}^{(t-1)} | \tilde{\xi}^*)}{|\hat{E}| \pi(\tilde{\xi}^{(t-1)}) q(\tilde{\xi}^* | \tilde{\xi}^{(t-1)})} \right\}$ 
16:  Else  $\tilde{\xi}^{(t)} \leftarrow \tilde{\xi}^{(t-1)}$  and  $\mathcal{S}_\xi^{(t)} \leftarrow \mathcal{S}_\xi^{(t-1)}$ 
17:  Draw  $\phi^*$  from  $q(\phi | \phi^{(t-1)})$ 
18:  Compute GP predictive means  $c_n^*$  and control variates:  $l_n = l(y_n | c_n^*, \rho^{(t)})$ 
19:    for  $n = 1, \dots, N$ 
20:  Sample a block  $g$  and random variates  $\mathcal{V}_g^*$ .
21:  Compute  $\log(|\hat{E}^*|)$  using Eq. (9)
22:  Set  $\phi^{(t)} \leftarrow \phi^*$ ;  $\mathcal{V}_g \leftarrow \mathcal{V}_g^*$ ;  $\log(|\hat{E}|) \leftarrow \log(|\hat{E}^*|)$ ;  $\mathcal{S}_\phi^{(t)} \leftarrow \text{sign}(\hat{E}^*)$ ; and
23:     $c_{1:N} \leftarrow c_{1:N}^*$  with probability:  $\min \left\{ 1, \frac{|\hat{E}^*| \pi(\phi^*) q(\phi^{(t-1)} | \phi^*)}{|\hat{E}| \pi(\phi^{(t-1)}) q(\phi^* | \phi^{(t-1)})} \right\}$ 
24:  Else  $\phi^{(t)} \leftarrow \phi^{(t-1)}$  and  $\mathcal{S}_\phi^{(t)} \leftarrow \mathcal{S}_\phi^{(t-1)}$ 
25: end for
    
```

3.2 Signed block PM MCMC

The algorithm is a simple extension of the signed dependent PM scheme developed in Quiroz et al. [2020], using a Metropolis-within-Gibbs (MwG) sampler to iterate over the components $(\tilde{\xi}, \rho, \phi)$.

Sign correction. In order to employ the block-Poisson estimator, one must define a lower bound a for \hat{d}_B . Quiroz et al. [2020, Section 3.3] explain that employing a soft lower bound, i.e. a lower bound that makes $\tau = \Pr(\hat{E} \geq 0) \approx 1$, is computationally more efficient than employing a strict lower bound. One can then use the absolute value of \hat{E} to avoid possible negative likelihood estimates and apply a sign correction to obtain asymptotically exact estimates from the MCMC samples [Lyne et al., 2015].

Block correlation. A key advantage of the estimator in Eq. (9) is that through blocking structure, an efficient correlated PM scheme can be constructed. Specifically, at each step, we only update the random variables $\mathcal{V}_g = (\mathcal{H}_g, (\alpha_1^{h,g}, \dots, \alpha_B^{h,g}, \xi_1^{h,g}, \dots, \xi_B^{h,g})_{h=1}^{\mathcal{H}_g})$ of a single block g , drawn uniformly from 1 to κ . The remaining random variables of all other blocks are fixed. As shown in Quiroz et al. [2020], this induces the correlation $\rho = \text{Cor}(\log|\hat{E}^*|, \log|\hat{E}|) \approx 1 - 1/\kappa$ between the log of the estimated likelihood at the proposed and current states.

Moreover, one can target a prespecified correlation $\rho \approx 1 - 1/G$ by grouping the κ Poisson estimators into a corresponding number of groups, G .

Metropolis-within-Gibbs We employ an MwG framework to sample the parameters $(\tilde{\xi}, \rho, \phi)$. The whitened parameters $\tilde{\xi}$ may be sampled via elliptical slice sampling [ELLSS, Murray et al., 2010], preconditioned Crank-Nicolson [Cotter et al., 2013], or recent adaptive extensions [Wallin and Vadlamani, 2018]. For example, for the two-level GP model in Section 4.3, we employ independent Metropolis-Hastings (MH) at the first level and ELLSS at the second level. An adaptive random walk [Roberts and Rosenthal, 2009] may be used for the likelihood parameters ρ and GP hyperparameters ϕ . Alternatively, Hamiltonian Monte Carlo samplers may be employed, following Dang et al. [2019].

Algorithm 1 summarizes the PM scheme. It requires prespecification of the algorithmic parameters (κ, a, B) as well as the inducing locations \tilde{X} , which are discussed in the following subsections.

3.3 Algorithmic parameters

We follow the guidelines of Quiroz et al. [2020] to optimally select the key algorithmic parameters, namely the lower bound a , the number of Poisson estimators κ , and the number of subsamples B . First, by minimising the variance of the estimator, the authors suggest the lower bound $a = \bar{d} - \kappa$, where \bar{d} is an approximation of the difference d . Next, they set κ and B by minimising a measure of computational time (CT). This quantity describes the cost required to produce an estimator of equivalent precision as that based on a single Monte Carlo draw from the target and is derived under a normality assumption for \hat{d}_B . The measure balances the inefficiency of the MCMC (IF), the computational cost of the likelihood evaluation, and the probability of a negative likelihood estimate and is defined as:

$$\text{CT} = (NM + \kappa BM^2 + M^3) \frac{\text{IF}}{(2\tau - 1)^2}. \quad (10)$$

Expressions for IF and τ are provided in Quiroz et al. [2020], and approximations can be obtained given the values of κ , B , γ , and ρ . We note that IF and τ , and in general quantities such as γ and E , are conditioned on the values of the state, but to simplify notation we suppress this dependency.

Algorithm 2 details the steps required to obtain the optimal tuning parameters (\bar{d}, κ, B) . At the first step, in order to obtain an approximation of the difference \bar{d} and an estimate of γ , we run a pilot MCMC to generate a small number of approximate samples, S , from the posterior of interest based on a subsample. To do so, one can employ a Taylor expansion or Gauss-Hermite quadrature to approximate the intractable likelihood. We employ a conservative estimate of γ that is the maximum of the estimated $\hat{\gamma}^{(s)}$ across the pilot MCMC draws. Next, the optimal κ is obtained based on a grid search to minimise the CT in Eq (10), computed based on our estimate of γ and for a fixed value of subsamples B . In general, the number of subsamples B can also be optimized, but Quiroz et al. [2020] instead recommend setting $B = 30$, thus dedicating more computational resources to more batches over larger batch sizes.

3.4 Inducing points

A poor selection of the inducing points can lead to unsatisfactory posterior and predictive estimates. While a strategy based on K-means clustering of the inputs is fast and computationally cheap, Hensman et al. [2015] demonstrate that significant improvements can be achieved by optimizing the inducing points. Specifically, following Hensman et al. [2015], the inducing points can be optimized based on an initial Gaussian approximation to the posterior, prior to running the MCMC. Recently, Rossi et al. [2020] advocate for a fully Bayesian treatment of the inducing points in approximations based on fully independent training conditionals [FITC, Quiñonero-Candela and Rasmussen, 2005]. Beyond this, Uhlenholt et al. [2020] place a point process prior on the inducing points, to learn not only the locations but also the number of inducing points. Extending and incorporating these advancements within our scheme is a promising direction of research.

To select the number of inducing points, a common approach is to increase M until there is no improvement in an approximation to the marginal likelihood. Indeed, this is typically the case in variational inference when one aims to optimize a lower bound on the marginal likelihood. Burt et al. [2019] study convergence rates of variationally sparse GP regression to provide asymptotic guidelines for the choice of M . For example, they show that with the squared exponential kernel, it suffices to take $M = \mathcal{O}(\log^D(N))$. Alternatively, we discuss in Appendix A.5 an heuristic approach to select the number of inducing points select the number of inducing points by optimizing a measure that combines both accuracy and computational cost.

Algorithm 2 Optimal tuning parameters for S-BP-PM

Require: Target distribution: $q(\tilde{\xi}, \rho, \phi)$, small number of samples: S , subsample size: B' , batch size B , a grid of κ values, assumption: $\hat{d}_B^{h,k} \stackrel{\text{iid}}{\sim} N(d, \gamma/B)$.

- 1: Run pilot MCMC with approximated likelihood (e.g. Gauss-Hermite or Taylor) to produce S samples from $q(\tilde{\xi}, \rho, \phi)$ based on a subsample.
 - 2: **for** $s = 1, \dots, S$ **do**
 - 3: **for** $b = 1, \dots, B'$ **do**
 - 4: Sample $\alpha_b \sim \text{Unif}(1, \dots, N)$
 - 5: Sample $z_{\alpha_b} \sim N(c_{\alpha_b}, w_{\alpha_b}^2)$ where

$$c_{\alpha_b} = C_{z_{\alpha_b}, \tilde{z}}(C_{\tilde{z}, \tilde{z}})^{-1} L(\phi^{(s)}) \tilde{\xi}^{(s)},$$

$$w_{\alpha_b}^2 = C_{z_{\alpha_b}, z_{\alpha_b}} - C_{z_{\alpha_b}, \tilde{z}}(C_{\tilde{z}, \tilde{z}})^{-1} C_{\tilde{z}, z_{\alpha_b}}$$
 - 6: Compute $\nu_{\alpha_b}^{(s)}(z_{\alpha_b}) = l(y_{\alpha_b} | c_{\alpha_b}, \rho^{(s)}) + (z_{\alpha_b} - c_{\alpha_b}) l'(y_{\alpha_b} | c_{\alpha_b}, \rho^{(s)})$
 - 7: Evaluate: $\hat{d}_{\alpha_b}^{(s)} = l(y_{\alpha_b} | z_{\alpha_b}, \rho^{(s)}) - \nu_{\alpha_b}^{(s)}(z_{\alpha_b})$
 - 8: **end for**
 - 9: Compute: $\hat{\sigma}^{2(s)} = \frac{1}{B'-1} \sum_{b=1}^{B'} \left(\hat{d}_{\alpha_b}^{(s)} - \frac{1}{B'} \sum_{b=1}^{B'} \hat{d}_{\alpha_b}^{(s)} \right)^2$
 - 10: Compute: $\hat{\gamma}^{(s)} = N^2 \hat{\sigma}^{2(s)}$
 - 11: Compute $\hat{d}_{B'}^{(s)} = \frac{N}{B'} \sum_{b=1}^{B'} \hat{d}_{\alpha_b}^{(s)}$
 - 12: **end for**
 - 13: Set $\gamma_{max} = \max \hat{\gamma}^{(s)}$
 - 14: Compute $\bar{d} = \frac{1}{S} \sum_{s=1}^S \hat{d}_{B'}^{(s)}$
 - 15: **for each** κ **do**
 - 16: Compute: $\sigma_{\log|\hat{E}|}^2 = \kappa(v^2 + \eta^2)$ with ▷ Approximate expectations by truncation

$$v = \log \left(\sqrt{\frac{\gamma_{max}}{B\kappa^2}} \right) + \frac{1}{2} \left(\log 2 + \mathbb{E}_p[\psi^{(0)}(1/2 + p)] \right),$$

$$\eta^2 = \frac{1}{4} \left(\mathbb{E}_p[\psi^{(1)}(1/2 + p)] + \mathbb{V}_p[\psi^{(1)}(1/2 + p)] \right),$$
 - where $p \sim \text{Pois}(B\kappa^2/2\gamma_{max})$, and $\psi^{(i)}$ the polygamma function of order i .
 - 17: Compute the probability of a positive \hat{E} : ▷ Φ denotes CDF of a standard Gaussian

$$\tau = \frac{1}{2} \left(1 + \exp \left[2\kappa \left(\Phi \left(\frac{\kappa\sqrt{B}}{\sqrt{\gamma_{max}}} \right) - 1 \right) \right] \right)$$
 - 18: **if** $\kappa < 100$ **then** $\rho = 1 - \frac{1}{\kappa}$ **else** $\rho = 1 - \frac{1}{100}$ **end if**
 - 19: Employ GH quadrature to approximate: ▷ $f \sim N \left(\frac{1}{2} \sigma_{\log|\hat{E}|}^2, \sigma_{\log|\hat{E}|}^2 \right)$

$$\hat{\mathbb{E}}_f \approx \mathbb{E}_f \left(\frac{1 - \vartheta}{\vartheta} \right), \quad \vartheta = \exp(-\beta + \omega^2/2) \Phi \left(\frac{\beta}{\omega} - \omega \right) + \Phi \left(\frac{-\beta}{\omega} \right),$$

with $\beta := f + \sigma_{\log|\hat{E}|}^2$, $\omega = \sigma_{\log|\hat{E}|} (1 - \rho^2)^{1/2}$.
 - 20: Compute the inefficiency: $\text{IF} = 1 + 2\hat{\mathbb{E}}_f$
 - 21: Compute the computational time:

$$\text{CT}^* = (\kappa B M^2 + N M + M^3) \frac{\text{IF}}{(2\tau - 1)^2}$$
 - 22: **end for**
 - 23: **return** κ with the minimum CT^* and \bar{d} .
-

3.5 Posterior and predictive estimates

Note that the block-Poisson estimator in Eq. (9) is only unbiased without the absolute value. Therefore, MCMC draws $(\tilde{\xi}, \rho, \phi)$ do not follow $q(\tilde{\xi}, \rho, \phi)$, but rather

$$\check{q}(\tilde{\xi}, \rho, \phi) \propto \int \left| \hat{E} \right| \pi(\tilde{\xi}, \rho, \phi) \pi(\mathcal{V}_1, \dots, \mathcal{V}_G) d\mathcal{V}_1, \dots, \mathcal{V}_G,$$

where $\pi(\tilde{\xi}, \rho, \phi)$ is the prior over $(\tilde{\xi}, \rho, \phi)$ and $\pi(\mathcal{V}_1, \dots, \mathcal{V}_G)$ is the density of the auxiliary random variables involved in computation of the block-Poisson estimator. Nevertheless, one can estimate expectations with respect to $q(\tilde{\xi}, \rho, \phi)$ by taking the MCMC draws from $\check{q}(\tilde{\xi}, \rho, \phi)$ and applying an importance sampling step that corrects for the sign of the estimator [Lyne et al., 2015]. For instance, assume one wants to compute the expectation of some function $g(\Psi)$ depending on a subset Ψ of the parameters $(\rho, \tilde{\xi}, \phi)$. Then,

$$\mathbb{E}_q[g(\Psi)] = \frac{\mathbb{E}_{\check{q}}[g(\Psi)\mathcal{S}]}{\mathbb{E}_{\check{q}}[\mathcal{S}]},$$

with $\mathcal{S} = \text{sign}(\hat{E})$. Thus, one can estimate $\mathbb{E}_q[g(\Psi)]$ through

$$\mathbb{E}_q[g(\Psi)] \approx \frac{\sum_{t=1}^T \sum_{j=1}^J \mathcal{S}_j^{(t)} g(\Psi_j^{(t)})}{\sum_{t=1}^T \sum_{j=1}^J \mathcal{S}_j^{(t)}},$$

where $\Psi_j^{(t)}$ and $\mathcal{S}_j^{(t)}$ denote the state and sign, respectively, at iteration t when updating the j th parameter of Ψ in the corresponding Gibbs step. As an example, the prediction of the unknown function at a location x^* is given by $\mathbb{E}[z^* | \mathcal{D}] = \mathbb{E}_q[\mathbb{E}[z^* | \tilde{\xi}, \phi]]$, and thus can be computed by setting $g(\tilde{\xi}, \phi) = \mathbb{E}[z^* | \tilde{\xi}, \phi]$ to be the GP prior predictive mean.

In addition, while credible intervals reflecting uncertainty cannot be directly computed from the MCMC output, one can estimate the posterior probability that the parameters belong to a specified region, which in turn can be used to compute credible intervals. For example, considering z^* , let $g(\tilde{\xi}, \phi) = F_{z^*}(z | \tilde{\xi}, \phi)$ be the CDF of the Gaussian prior predictive of z^* evaluated at any $z \in \mathbb{R}$, then

$$\Pr(z^* \leq z | \mathcal{D}) \approx \frac{\sum_{t=1}^T \mathcal{S}_{\tilde{\xi}}^{(t)} F_{z^*}(z | \tilde{\xi}^{(t)}, \phi^{(t-1)}) + \mathcal{S}_{\phi}^{(t)} F_{z^*}(z | \tilde{\xi}^{(t)}, \phi^{(t)})}{\sum_{t=1}^T \mathcal{S}_{\tilde{\xi}}^{(t)} + \mathcal{S}_{\phi}^{(t)}}.$$

By evaluating this over a grid of z values, one can then compute credible intervals from the CDF.

4 Motivating model: two-level non-stationary GP regression

Many statistical and machine learning tasks focus on parametric, stationary covariance functions, largely due to computational convenience. However, this assumption is rarely realistic in practice, and as a consequence, various approaches exist to account for non-stationarity [e.g. Kim et al., 2005, Montagna and Tokdar, 2016, Volodina and Williamson, 2020]. We focus on the the family of non-stationary covariance functions introduced by Paciorek and Schervish [2006],

$$C_{\phi}^{\text{NS}}(\mathbf{x}_n, \mathbf{x}_{n'}) = \tau_z^2 \frac{|\Sigma(\mathbf{x}_n)|^{\frac{1}{4}} |\Sigma(\mathbf{x}_{n'})|^{\frac{1}{4}}}{|\Sigma(\mathbf{x}_n) + \Sigma(\mathbf{x}_{n'})|/2|^{\frac{1}{2}}} R_{\psi}(Q_{nn'}), \quad (11)$$

with $Q_{nn'} = \sqrt{(\mathbf{x}_n - \mathbf{x}_{n'})^T ((\Sigma(\mathbf{x}_n) + \Sigma(\mathbf{x}_{n'}))/2)^{-1} (\mathbf{x}_n - \mathbf{x}_{n'})}$, R_{ψ} a stationary correlation function on \mathbb{R} , and $\Sigma(\cdot)$ a $D \times D$ spatially varying covariance matrix, referred to as the kernel matrix. Thus, the parameters ϕ of this nonparametric covariance function consist of the magnitude, τ_z^2 ; the spatially varying covariance matrices, $\Sigma(\cdot)$; and any additional parameters ψ of the stationary correlation function R_{ψ} . Importantly, non-stationarity is introduced through the kernel matrices, and these parameters must be inferred at every observed location. To control the number of parameters, one can place assumptions on the kernel matrix and type of non-stationary present. Here, we focus on a non-stationary isotropic covariance function, which is obtained by assuming the kernel matrices are scaled identity matrices such that $\Sigma(\cdot) = \ell^2(\cdot) I_D$. In this case, we can allow the spatially varying length-scale to be a function of the full D -dimensional input, with $\mathcal{O}(D)$ hyperparameters. Therefore, the kernel can be written as,

$$C_{\phi}^{\text{NS}}(\mathbf{x}_n, \mathbf{x}_{n'}) = \tau_z^2 \frac{\ell(\mathbf{x}_n)^{\frac{D}{2}} \ell(\mathbf{x}_{n'})^{\frac{D}{2}}}{([\ell^2(\mathbf{x}_n) + \ell^2(\mathbf{x}_{n'})]/2)^{\frac{D}{2}}} R_{\psi} \left(\sqrt{\frac{\sum_{d=1}^D (x_{nd} - x_{n'd})^2}{[\ell^2(\mathbf{x}_n) + \ell^2(\mathbf{x}_{n'})]/2}} \right). \quad (12)$$

In the two-level non-stationary GP model, we model the log transformed length-scale process with a stationary GP prior; that is, $u(\cdot) := \log(\ell(\cdot)) \sim \text{GP}(\mu_u, C_\varphi^s(\cdot, \cdot))$. This provides a flexible model, where information can be borrowed across neighboring observations to learn the local length scales at each location. While we focus on the two-level formulation, we highlight that deeper constructions with multiple levels of GPs can provide even more flexible non-stationary behavior [Dunlop et al., 2018]. The hierarchical formulation of the two-level regression model is:

$$\begin{aligned} y_n &\sim \text{N}(z(\mathbf{x}_n), \sigma_\varepsilon^2), \quad n = 1, \dots, N \\ z(\cdot) &\sim \text{GP}(0, C_\phi^{\text{NS}}) \\ u(\cdot) &:= \log(\ell(\cdot)) \sim \text{GP}(\mu_u, C_\varphi^s(\cdot, \cdot)) \\ (\sigma_\varepsilon^2, \tau_z^2, \psi, \varphi) &\sim \pi(\sigma_\varepsilon^2)\pi(\tau_z^2)\pi(\psi)\pi(\varphi). \end{aligned} \tag{13}$$

The sparse variational strategy is well-suited for this model because the complexity, in both the number of parameters and high correlation among them, makes (i) standard mean-field variational methods, which make strong independence assumptions, unsuitable and (ii) MCMC inference over the true posterior computationally expensive and challenging [Monterrubio-Gómez et al., 2020].

4.1 Variationally sparse two-level GP regression

We now derive the optimal sparse variational posterior for the two-level GP regression model. First, we augment the model with the inducing points $\tilde{\mathbf{X}} = (\tilde{\mathbf{x}}_1, \dots, \tilde{\mathbf{x}}_M)^T$ and, in addition to the inducing variables $\tilde{\mathbf{z}} = (z(\tilde{\mathbf{x}}_1), \dots, z(\tilde{\mathbf{x}}_M))^T$, we collect the values of the log length-scale process at the inducing points into the vector $\tilde{\mathbf{u}} = (u(\tilde{\mathbf{x}}_1), \dots, u(\tilde{\mathbf{x}}_M))^T$. Letting $\mathbf{u} = (u_1, \dots, u_N)^T$ denote the the log length-scale process at the observed locations, the joint prior is:

$$\pi(\mathbf{u}, \tilde{\mathbf{u}} \mid \varphi) = \text{N}(\mathbf{u} \mid \boldsymbol{\mu}_u^*, \boldsymbol{\Omega}_u) \text{N}(\tilde{\mathbf{u}} \mid \boldsymbol{\mu}_u, C_{\tilde{\mathbf{u}}, \tilde{\mathbf{u}}}^s),$$

where $\boldsymbol{\mu}_u$ denotes an M -dimensional vector with entries μ_u , $\boldsymbol{\mu}_u^* = \boldsymbol{\mu}_u + C_{\mathbf{u}, \tilde{\mathbf{u}}}^s (C_{\tilde{\mathbf{u}}, \tilde{\mathbf{u}}}^s)^{-1} (\tilde{\mathbf{u}} - \boldsymbol{\mu}_u)$, and $\boldsymbol{\Omega}_u = C_{\mathbf{u}, \mathbf{u}}^s - C_{\mathbf{u}, \tilde{\mathbf{u}}}^s (C_{\tilde{\mathbf{u}}, \tilde{\mathbf{u}}}^s)^{-1} C_{\tilde{\mathbf{u}}, \mathbf{u}}^s$. Additionally,

$$\pi(\mathbf{z}, \tilde{\mathbf{z}} \mid \mathbf{u}, \tilde{\mathbf{u}}, \tau_z^2, \psi) = \text{N}(\mathbf{z} \mid \boldsymbol{\mu}_z^*, \boldsymbol{\Omega}_z) \text{N}(\tilde{\mathbf{z}} \mid 0, C_{\tilde{\mathbf{z}}, \tilde{\mathbf{z}}}^{\text{NS}}),$$

with $\boldsymbol{\mu}_z^* = C_{\mathbf{z}, \tilde{\mathbf{z}}}^{\text{NS}} (C_{\tilde{\mathbf{z}}, \tilde{\mathbf{z}}}^{\text{NS}})^{-1} \tilde{\mathbf{z}}$ and $\boldsymbol{\Omega}_z = C_{\mathbf{z}, \mathbf{z}}^{\text{NS}} - C_{\mathbf{z}, \tilde{\mathbf{z}}}^{\text{NS}} (C_{\tilde{\mathbf{z}}, \tilde{\mathbf{z}}}^{\text{NS}})^{-1} C_{\tilde{\mathbf{z}}, \mathbf{z}}^{\text{NS}}$. The approximate variational posterior is assumed to take the form:

$$q(\mathbf{z}, \tilde{\mathbf{z}}, \mathbf{u}, \tilde{\mathbf{u}}, \boldsymbol{\theta}) \propto \pi(\mathbf{z} \mid \tilde{\mathbf{z}}, \mathbf{u}, \tilde{\mathbf{u}}, \boldsymbol{\theta}) \pi(\mathbf{u} \mid \tilde{\mathbf{u}}, \boldsymbol{\theta}) q(\tilde{\mathbf{z}}, \tilde{\mathbf{u}}, \boldsymbol{\theta}),$$

where $\boldsymbol{\theta} := \{\sigma_\varepsilon^2, \tau_z^2, \psi, \varphi\}$. By minimizing the KL divergence (see Appendix A), we obtain the optimal variational posterior:

$$q(\tilde{\mathbf{z}}, \tilde{\mathbf{u}}, \boldsymbol{\theta}) \propto \exp \left(\sum_{n=1}^N \mathbb{E}_{(z_n, u_n)} [\log(\text{N}(y_n \mid z_n, \sigma_\varepsilon^2))] \right) \pi(\tilde{\mathbf{z}} \mid \tilde{\mathbf{u}}, \boldsymbol{\theta}) \pi(\tilde{\mathbf{u}} \mid \boldsymbol{\theta}) \pi(\boldsymbol{\theta}), \tag{14}$$

where the expectation is taken with respect to $\pi(z_n, u_n \mid \tilde{\mathbf{z}}, \tilde{\mathbf{u}}, \boldsymbol{\theta})$. The elements of the expected log-likelihood in Eq. (14) can be written as

$$\mathbb{E}_{(z_n, u_n)} [\log(\text{N}(y_n \mid z_n, \sigma_\varepsilon^2))] = \mathbb{E}_{u_n} [l(y_n \mid u_n, \tilde{\mathbf{z}}, \boldsymbol{\theta})],$$

where we define

$$\begin{aligned} l(y_n \mid u_n, \tilde{\mathbf{z}}, \boldsymbol{\theta}) &= \mathbb{E}_{z_n} [\log(\text{N}(y_n \mid z_n, \sigma_\varepsilon^2)) \mid u_n] \\ &= -\frac{1}{2} \log(2\pi\sigma_\varepsilon^2) - \frac{1}{2\sigma_\varepsilon^2} [(y_n - \mathbb{E}_{z_n}[z_n \mid u_n])^2 + V_{z_n}(z_n \mid u_n)] \\ &= -\frac{1}{2} \log(2\pi\sigma_\varepsilon^2) - \frac{1}{2\sigma_\varepsilon^2} [(y_n - C_{\mathbf{z}, \tilde{\mathbf{z}}}^{\text{NS}} (C_{\tilde{\mathbf{z}}, \tilde{\mathbf{z}}}^{\text{NS}})^{-1} \tilde{\mathbf{z}})^2 + \tau_z^2 - C_{\mathbf{z}, \tilde{\mathbf{z}}}^{\text{NS}} (C_{\tilde{\mathbf{z}}, \tilde{\mathbf{z}}}^{\text{NS}})^{-1} C_{\tilde{\mathbf{z}}, \mathbf{z}}^{\text{NS}}]. \end{aligned}$$

We intend to explore the variational posterior in Eq. (14) using MCMC, however the required expectations of $l(y_n \mid u_n, \tilde{\mathbf{z}}, \boldsymbol{\theta})$ with respect to $\pi(u_n \mid \tilde{\mathbf{u}}, \boldsymbol{\theta})$ are intractable. To overcome this, in the following subsections, we first present and discuss the limitations of a Gauss-Hermite approach and then describe the PM scheme.

4.2 Gauss-Hermite approach

Following Hensman et al. [2015], the intractable expectations can be approximated with Gaussian-Hermite quadrature. In this case, to improve the approximation and mixing, we rewrite the expected log-likelihood as:

$$\begin{aligned} \mathbb{E}_{u_n}[l(y_n|u_n, \tilde{\mathbf{z}}, \boldsymbol{\theta})] &= -\frac{1}{2} \log(2\pi\sigma_\varepsilon^2) - \frac{1}{2\sigma_\varepsilon^2} [(y_n - \beta_n(C_{\tilde{\mathbf{z}}, \tilde{\mathbf{z}}}^{\text{NS}})^{-1}\tilde{\mathbf{z}})^2 + \tau_z^2 - \alpha_n] \\ &\quad - \frac{1}{2\sigma_\varepsilon^2} [\tilde{\mathbf{z}}^T (C_{\tilde{\mathbf{z}}, \tilde{\mathbf{z}}}^{\text{NS}})^{-1} (\mathbf{P}_n - \beta_n^T \beta_n) (C_{\tilde{\mathbf{z}}, \tilde{\mathbf{z}}}^{\text{NS}})^{-1} \tilde{\mathbf{z}}], \end{aligned}$$

where we denote the required intractable expectations by

$$\begin{aligned} \beta_n &= \mathbb{E}_{u_n} [C_{z_n, \tilde{\mathbf{z}}}^{\text{NS}}], \\ \mathbf{P}_n &= \mathbb{E}_{u_n} [C_{\tilde{\mathbf{z}}, z_n}^{\text{NS}} C_{z_n, \tilde{\mathbf{z}}}^{\text{NS}}], \end{aligned} \tag{15}$$

and define

$$\alpha_n = \mathbb{E}_{u_n} [C_{z_n, \tilde{\mathbf{z}}}^{\text{NS}} (C_{\tilde{\mathbf{z}}, \tilde{\mathbf{z}}}^{\text{NS}})^{-1} C_{\tilde{\mathbf{z}}, z_n}^{\text{NS}}] = \sum_{i,j=1}^M ((C_{\tilde{\mathbf{z}}, \tilde{\mathbf{z}}}^{\text{NS}})^{-1} \odot \mathbf{P}_n)_{ij},$$

with \odot denoting the Hadamard product. Importantly, this allows us to marginalise the latent variables $\tilde{\mathbf{z}}$. Furthermore, we employ whitening to break the correlation between $\tilde{\mathbf{u}}$ and $\boldsymbol{\varphi}$, defining $\tilde{\mathbf{u}} = L(\boldsymbol{\varphi})\tilde{\boldsymbol{\zeta}} + \boldsymbol{\mu}_u$, where $\tilde{\boldsymbol{\zeta}} \sim \text{N}(0, I_M)$ and $L(\boldsymbol{\varphi})L(\boldsymbol{\varphi})^T = C_{\tilde{\mathbf{u}}, \tilde{\mathbf{u}}}^{\text{S}}$. Consequently, our MCMC scheme aims to simulate from the whitened marginal variational posterior,

$$\begin{aligned} q(\tilde{\boldsymbol{\zeta}}, \boldsymbol{\theta}) &\propto \text{N}(\tilde{\boldsymbol{\zeta}} | 0, I_M) \pi(\boldsymbol{\theta}) \sigma_\varepsilon^{-N} \exp \left(-\frac{1}{2\sigma_\varepsilon^2} \sum_{n=1}^N [y_n^2 + \tau_z^2 - \alpha_n] \right) \times \\ &\quad \left[\frac{|C_{\tilde{\mathbf{z}}, \tilde{\mathbf{z}}}^{\text{NS}}|^{\frac{1}{2}}}{|C_{\tilde{\mathbf{z}}, \tilde{\mathbf{z}}}^{\text{NS}} + \sigma_\varepsilon^{-2} \mathbf{P}|^{\frac{1}{2}}} \exp \left(\frac{1}{2\sigma_\varepsilon^4} \mathbf{y}^T B (C_{\tilde{\mathbf{z}}, \tilde{\mathbf{z}}}^{\text{NS}} + \sigma_\varepsilon^{-2} \mathbf{P})^{-1} B^T \mathbf{y} \right) \right]_{\tilde{\mathbf{u}}}, \end{aligned} \tag{16}$$

where $\tilde{\mathbf{u}}$ is replaced by $L(\boldsymbol{\varphi})\tilde{\boldsymbol{\zeta}} + \boldsymbol{\mu}_u$ in the expression in brackets; B an $N \times M$ matrix with rows β_n ; and $\mathbf{P} = \sum_{n=1}^N \mathbf{P}_n$. Furthermore, when required, we can sample $\tilde{\mathbf{z}}$ from its conditional variational posterior:

$$\tilde{\mathbf{z}} | \tilde{\mathbf{u}}, \boldsymbol{\theta} \sim \text{N} \left(\sigma_\varepsilon^{-2} C_{\tilde{\mathbf{z}}, \tilde{\mathbf{z}}}^{\text{NS}} (C_{\tilde{\mathbf{z}}, \tilde{\mathbf{z}}}^{\text{NS}} + \sigma_\varepsilon^{-2} \mathbf{P})^{-1} B^T \mathbf{y}, C_{\tilde{\mathbf{z}}, \tilde{\mathbf{z}}}^{\text{NS}} (C_{\tilde{\mathbf{z}}, \tilde{\mathbf{z}}}^{\text{NS}} + \sigma_\varepsilon^{-2} \mathbf{P})^{-1} C_{\tilde{\mathbf{z}}, \tilde{\mathbf{z}}}^{\text{NS}} \right). \tag{17}$$

Full details of the algorithm employed are given in the Supplementary Material. At each step, the cost of single likelihood evaluation is dominated by approximation of the intractable integrals, namely, the elements of β_n and \mathbf{P}_n for each data point $n = 1, \dots, N$. This results in a computational complexity of $\mathcal{O}(JNM^2)$ per expected log-likelihood evaluation, in contrast to $\mathcal{O}(N^3)$ for evaluation of the true likelihood.

Clearly, the quadrature order J can have a strong impact on the computational complexity; moreover, a large J may be required for sufficient approximations. Here we analyse the integrand that corresponds to β_n for the non-stationary squared exponential (SE) kernel. Figure 1 illustrates how the shape of the integrand varies for different δ values, with δ representing the distance between two locations, and fixed hyperparameters. We can observe how the position of the nodes often misses the peak. Also, as we increase δ , the function becomes sharper, and how fast this occurs is determined by the hyperparameters. Figure 1(f) illustrates clearly why the approximation can be poor, even with several nodes. We also highlight that in some cases, the node positions are located in regions where the function is flat, see for instance Figure 1(h), which should depict ten horizontal bars but only two can be observed.

4.3 Pseudo-marginal approach

To address the shortcomings of the Gauss-Hermite approach, we employ the PM framework described in Section 3. In this case, we do not marginalize the inducing variables $\tilde{\mathbf{z}}$, in order to maintain the factorized form of log-likelihood required. In addition, to break the correlation, whitening is applied for both $\tilde{\mathbf{z}}$ and $\tilde{\mathbf{u}}$ based on the transformations: $\tilde{\mathbf{z}} = L(\tilde{\mathbf{u}})\tilde{\boldsymbol{\xi}}$ and $\tilde{\mathbf{u}} = L(\boldsymbol{\varphi})\tilde{\boldsymbol{\zeta}} + \boldsymbol{\mu}_u$, where $\tilde{\boldsymbol{\xi}} \sim \text{N}(0, I_M)$, $\tilde{\boldsymbol{\zeta}} \sim \text{N}(0, I_M)$, $L(\tilde{\mathbf{u}})L(\tilde{\mathbf{u}})^T = C_\phi^{\text{NS}}$ and $L(\boldsymbol{\varphi})L(\boldsymbol{\varphi})^T = C_\phi^{\text{S}}$. Thus, the whitened variational posterior has the form

$$q(\tilde{\boldsymbol{\xi}}, \tilde{\boldsymbol{\zeta}}, \boldsymbol{\theta}) \propto \left[\exp \left(\sum_{n=1}^N \mathbb{E}_{u_n}[l(y_n | u_n, \tilde{\mathbf{z}}, \boldsymbol{\theta})] \right) \right]_{\tilde{\mathbf{z}}, \tilde{\mathbf{u}}} \text{N}(\tilde{\boldsymbol{\xi}} | 0, I_M) \text{N}(\tilde{\boldsymbol{\zeta}} | 0, I_M) \pi(\boldsymbol{\theta}), \tag{18}$$

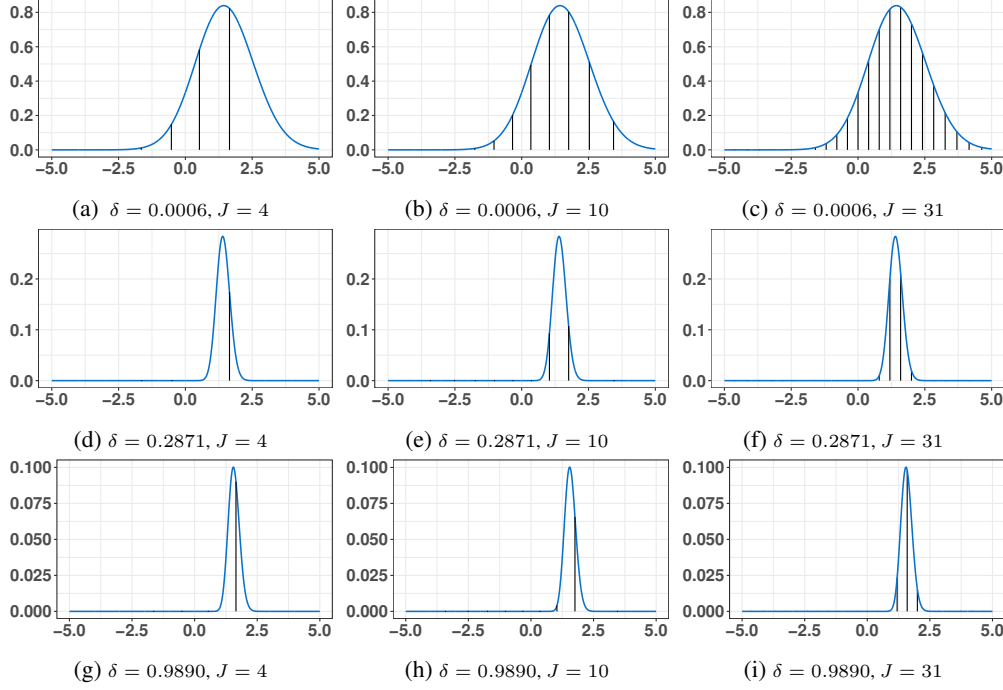


Figure 1: The effect of the number of integration points in Gauss-Hermite quadrature. The blue line denotes the integrand of β_n for the non-stationary SE kernel, with an SE kernel for $u(\cdot)$ with length-scale $\lambda = 0.1$. The vertical black lines depict the integrand evaluated at the node locations.

where \tilde{z} and \tilde{u} are replaced by $L(\tilde{u})\tilde{\xi}$ and $L(\varphi)\tilde{\zeta} + \mu_u$, respectively, in the expression in brackets.

To apply the PM scheme, we look for an unbiased estimator, \hat{E} , of the first term in the right hand side of eq. (18). Such estimator can be found by employing the doubly stochastic block-Poisson estimator in Definition 1. In this case, the control variates, $\bar{\nu}_n(u_n)$, is defined through a first-order Taylor-expansion around the mean of $\pi(u_n | \theta)$; such that,

$$\nu_n(u_n) = l(y_n | \mathbb{E}[u_n], \tilde{z}, \theta) + (\ell_n - \exp(\mathbb{E}[u_n]))l'(y_n | \mathbb{E}[u_n], \tilde{z}, \theta).$$

Note that the computational cost of the control variates is $\mathcal{O}(NM^2)$ and consequently, evaluation of the doubly stochastic block estimator is of order $\mathcal{O}(NM^2 + \kappa BM^2 + M^3)$. We emphasize that one can define alternative control variates of reduced computational complexity (see Appendix A.3). Details of the sampling algorithm for this approach are provided in Appendix A.7.

5 Simulation study

In the following synthetic dataset we compare the performance of the Gauss-Hermite approach from Section 4.2 and the proposed pseudo-marginal scheme described in Section 4.3. We aim to evaluate if the S-BP-PM algorithm performs better than the quadrature approach in (i) recovering the true parameters, (ii) predictive performance, and (iii) computational time. In addition, we provide a comparison with the full (non-sparse) model, to highlight the computational benefits of the sparse scheme.

Following Titsias [2009], we select the inducing points by maximising a lower bound to the sparse variational marginal likelihood of a stationary Gaussian process (which is available in closed form). More precisely, we employ a stationary Gaussian process with Matérn 3/2 covariance function and optimise the inducing points using the GPstuff toolbox implemented in MATLAB [Vanhatalo et al., 2015]. The optimised locations are then employed in the proposed MCMC schemes.

5.1 1-dimensional dataset

We simulate $N = 1,000$ observations from the two-level non-stationary GP model with domain $[0, 1]$, noise variance $\sigma_\varepsilon^2 = 0.02$, and stationary length-scale hyperparameter $\lambda = 0.1$. The results of the Gauss-Hermite scheme employ-

ing different numbers of inducing points ($M = 30, 45, 60$) and different quadrature orders ($J = 4, 5, 8, 10, 15$) are contrasted with those obtained with our proposed pseudo-marginal scheme.

5.1.1 Posterior inference

For the Gauss-Hermite approach, we employ the sampling scheme described in Appendix A.6 for $T = 50,000$ iterations, employing the same initialisations across the varying number of inducing points $M = 30, 45, 60$ and quadrature orders $J = 4, 5, 8, 10, 15$. The first 30,000 iterations are discarded as burnin.

For the S-BP-PM scheme, we first determine the optimal tuning parameters needed for the algorithm; namely, a , κ , and B . To do so, we investigate the normality assumption of the estimator $\hat{d}_{B=30}$ needed to employ Algorithm 2. (Figure 6 in the Appendix shows histograms of 500 estimators for $M = 30, 45$, and 60 confirming the assumption). The resulting optimal tuning parameters are also shown in Appendix B.1.1. We run the sampling scheme discussed in Appendix A.7 for $T = 50,000$ with burnin of 30,000, for $M = 30, 60$, and 40,000 for $M = 45$.

First, the posterior of the log noise variance indicate that the parameter can be greatly over-estimated, especially when using few inducing points (see Figure 2). This can be the result of underestimation of the posterior variance of the latent GP (and consequently, an overestimation of the noise variance to compensate [Gadd et al., 2018]). Second, posterior summaries of the length-scale process illustrated in Figure 3 highlight that increasing the number of inducing points and the number of nodes in the quadrature approximation does not necessarily result in more accurate posterior estimates (see Appendix B.1.2, Figure 7 for more details).

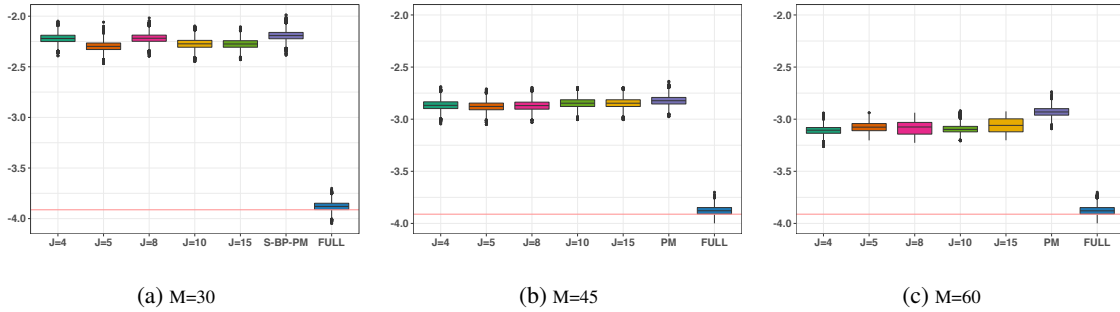


Figure 2: Boxplots of the MCMC samples for the logarithm of the noise variance parameter for different numbers of inducing points ($M = 30, 45, 60$). Each plot shows results with different quadrature orders ($J = 4, 5, 8, 10, 15$), the S-BP-PM scheme in purple and the full MCMC procedure in blue. The true parameter value is depicted in red.

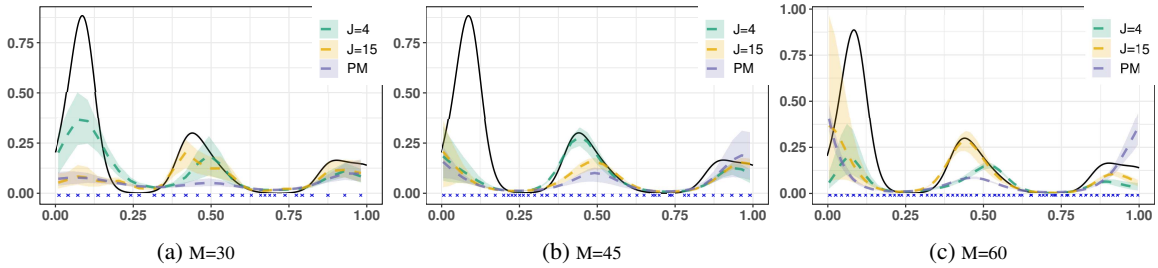


Figure 3: Posterior estimates for spatially varying parameter $\ell(\cdot)$. The black line denotes the true process. The colour-coded dashed lines show posterior estimates with 95% HPD credible intervals for $J = 4, 15$, and the S-BP-PM.

Figure 5(d) reports the computational time needed for inference with the S-BP-PM algorithm versus a full MCMC procedure and the Gauss-Hermite quadrature approach with the different number of nodes considered. Firstly, the figure highlights the clear computational benefit of employing the sparse variational posterior approximation. Secondly, we observe that our proposed S-BP-PM procedure with $M = 60$ is cheaper in comparison to the Gauss-Hermite approximation utilising $M = 30$ and only $J = 4$. This is relevant because this computational advantage will permit us to increase the number of inducing points, which is crucial to efficiently recover non-stationarities.

5.1.2 Predictions

To evaluate the predictive performance of the method, we make out-of-sample predictions at 300 locations. Figure 4 shows predictive estimates of the non-stationary latent function. It is clear that when there are not enough inducing points or when they are not well located, important features of the function can be missed, see for instance Figures 4(a) in the range $[0.1, 0.25]$ and compare with Figures 4(b)-(c). Moreover, for a fixed number and location of the inducing points, the order of the quadrature approximation also affects the results (see Appendix B.1.2, Figure 8 for more details). This is further emphasised in Figure 5, where, in some cases, the predictive error increases as we increase the number of nodes employed in the Gauss-Hermite approximation (see e.g. $J = 15$ for $M = 45$ in Figure 5(a)-(c)). Note also that with enough inducing points, e.g. $M = 60$ in this example, the quadrature order has less of an effect on the prediction errors. Importantly, when comparing the attained predictive performance of the S-BP-PM with the GH quadrature approach, we observe a slight reduction in point-wise errors, with more significant differences for the MAE (see Figure 5(a)-(b)). Finally, while we expect an underestimation in the posterior variance inherited from the variational distribution, we note that there is a small drop-off in EC when comparing the results of the GH quadrature (Figure 5(c)).

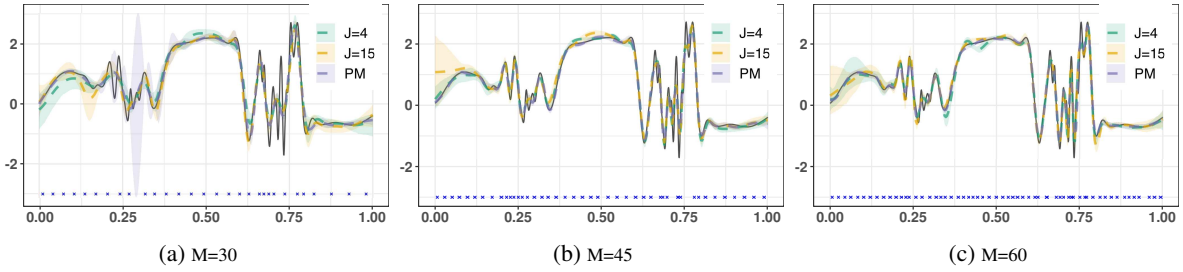


Figure 4: Out-of-sample predictions with different number of inducing points. The color-coded dashed lines denote the predictive mean with shaded areas depicting 95% HPD point-wise credible intervals. Solid black line denotes the true process.

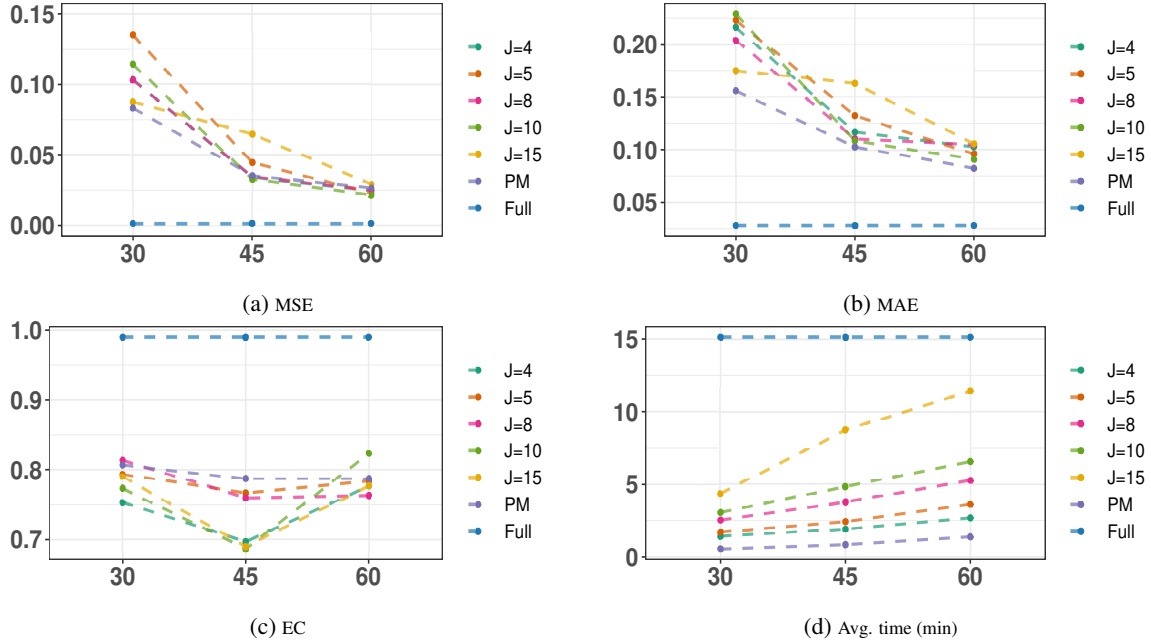


Figure 5: Comparison of the predictive performance and computational time. The results for S-BP-PM are shown in purple and compared with the Gauss-Hermite approximation approach with different number of nodes ($J = 4, 5, 8, 10, 15$) and the full (non-sparse) model. (a)-(c): Predictive performance comparison in terms of MSE, MAE and EC of out-of-sample predictions for different numbers of inducing points ($M = 30, 45, 60$). (d): Average computational time (in minutes) required for 100 MCMC iterations.

6 Discussion

We studied the MCMC for variationally sparse GPs approach introduced by Hensman et al. [2015], which due to its generality and computational benefits is an attractive framework to speed up GP inference. However, the necessity of approximating intractable expectations with Gauss-Hermite quadrature during likelihood evaluation can undermine the computational gains as some models might require high-order or multivariate GH quadrature approximations to explore the posterior efficiently. Instead, to avoid numerical integration, we propose a pseudo-marginal scheme, based on a doubly stochastic block-Poisson estimator, which permits asymptotically exact inference on complex models and large datasets, while also reducing the computational cost. In this paper, we demonstrate the advantages of our method on a 2-level GP regression model. However, we highlight that our approach applies to any GP based model, especially when the expected log-likelihood is not available in closed-form. Additionally, the proposed scheme can make use of parallel computations to further speed the inference procedure. Finally, we note that the computational benefits of the proposed pseudo-marginal scheme will be more evident in bigger datasets, higher dimensions, and/or deeper architectures.

References

- Christophe Andrieu, Gareth O Roberts, et al. The pseudo-marginal approach for efficient Monte Carlo computations. *The Annals of Statistics*, 37(2):697–725, 2009.
- Christophe Andrieu, Arnaud Doucet, and Roman Holenstein. Particle markov chain monte carlo methods. *Journal of the Royal Statistical Society: Series B (Statistical Methodology)*, 72(3):269–342, 2010.
- Ienkararan Arasaratnam, Simon Haykin, and Robert J Elliott. Discrete-time nonlinear filtering algorithms using gauss-hermite quadrature. *Proceedings of the IEEE*, 95(5):953–977, 2007.
- Sudipto Banerjee, Alan E Gelfand, Andrew O Finley, and Huiyan Sang. Gaussian predictive process models for large spatial data sets. *Journal of the Royal Statistical Society: Series B (Statistical Methodology)*, 70(4):825–848, 2008.
- Rémi Bardenet, Arnaud Doucet, and Chris Holmes. On markov chain monte carlo methods for tall data. *The Journal of Machine Learning Research*, 18(1):1515–1557, 2017.
- Mark A Beaumont. Estimation of population growth or decline in genetically monitored populations. *Genetics*, 164(3):1139–1160, 2003.
- Veronica J Berrocal, Adrian E Raftery, Tilmann Gneiting, and Richard C Steed. Probabilistic weather forecasting for winter road maintenance. *Journal of the American Statistical Association*, 105(490):522–537, 2010.
- David M Blei, Alp Kucukelbir, and Jon D McAuliffe. Variational inference: a review for statisticians. *Journal of the American Statistical Association*, 112(518):859–877, 2017.
- Alexander W Blocker. *fastGHQuad: Fast 'Rcpp' Implementation of Gauss-Hermite Quadrature*, 2018. URL <https://CRAN.R-project.org/package=fastGHQuad>. R package version 1.0.
- David Burt, Carl Edward Rasmussen, and Mark Van Der Wilk. Rates of convergence for sparse variational Gaussian process regression. In *International Conference on Machine Learning*, pages 862–871, 2019.
- S. L. Cotter, G. O. Roberts, A. M. Stuart, and D. White. Mcmc methods for functions: Modifying old algorithms to make them faster. *Statist. Sci.*, 28(3):424–446, 08 2013. doi: 10.1214/13-STS421. URL <https://doi.org/10.1214/13-STS421>.
- Noel Cressie and Gardar Johannesson. Fixed rank kriging for very large spatial data sets. *Journal of the Royal Statistical Society: Series B (Statistical Methodology)*, 70(1):209–226, 2008.
- Kurt Cutajar, Mark Pullin, Andreas Damianou, Neil Lawrence, and Javier González. Deep Gaussian processes for multi-fidelity modeling. 2019.
- Andreas Damianou and Neil Lawrence. Deep Gaussian processes. In *Artificial Intelligence and Statistics*, pages 207–215, 2013.
- Khue-Dung Dang, Matias Quiroz, Robert Kohn, Tran Minh-Ngoc, and Mattias Villani. Hamiltonian Monte Carlo with energy conserving subsampling. *Journal of Machine Learning Research*, 20:1–31, 2019.
- George Deligiannidis, Arnaud Doucet, and Michael K. Pitt. The correlated pseudomarginal method. *Journal of the Royal Statistical Society: Series B (Statistical Methodology)*, 80(5):839–870, 2018.
- A Doucet, MK Pitt, G Deligiannidis, and R Kohn. Efficient implementation of markov chain monte carlo when using an unbiased likelihood estimator. *Biometrika*, 102(2):295–313, 2015.

- Matthew M Dunlop, Mark Girolami, Andrew M Stuart, and Aretha L Teckentrup. How deep are deep Gaussian processes? *Journal of Machine Learning Research*, 19:1–46, 2018.
- Nicolas Durrande, Vincent Adam, Lucas Bordeaux, Stefanos Eleftheriadis, and James Hensman. Banded matrix operators for Gaussian Markov models in the automatic differentiation era. In *22nd International Conference on Artificial Intelligence and Statistics*, volume 89, pages 780–2789, 2019.
- Paul Fearnhead, Omiros Papaspiliopoulos, and Gareth O. Roberts. Particle filters for partially observed diffusions. *Journal of the Royal Statistical Society. Series B (Statistical Methodology)*, 70(4):755–777, 2008.
- Paul Fearnhead, Omiros Papaspiliopoulos, Gareth O. Roberts, and Andrew Stuart. Random-weight particle filtering of continuous time processes. *Journal of the Royal Statistical Society: Series B (Statistical Methodology)*, 72(4):497–512, 2010. doi: 10.1111/j.1467-9868.2010.00744.x. URL <https://rss.onlinelibrary.wiley.com/doi/abs/10.1111/j.1467-9868.2010.00744.x>.
- Maurizio Filippone. Bayesian inference for gaussian process classifiers with annealing and pseudo-marginal mcmc. In *2014 22nd International Conference on Pattern Recognition*, pages 614–619. IEEE, 2014.
- Maurizio Filippone and Mark Girolami. Pseudo-marginal Bayesian inference for Gaussian processes. *IEEE Transactions on Pattern Analysis and Machine Intelligence*, 36(11):2214–2226, 2014a.
- Maurizio Filippone and Mark Girolami. Pseudo-marginal bayesian inference for gaussian processes. *IEEE Transactions on Pattern Analysis and Machine Intelligence*, 36(11):2214–2226, 2014b.
- Charles Gadd, Sara Wade, Akeel Shah, and Dimitris Grammatopoulos. Pseudo-marginal bayesian inference for supervised gaussian process latent variable models. *arXiv preprint arXiv:1803.10746*, 2018.
- Charles Gadd, Sara Wade, and Alexis Boukouvalas. Enriched mixtures of generalised gaussian process experts. volume 108 of *Proceedings of Machine Learning Research*, pages 3144–3154, 2020.
- Walter Gautschi. A survey of gauss-christoffel quadrature formulae. In *EB Christoffel*, pages 72–147. Springer, 1981.
- Seymour Geisser and William F Eddy. A predictive approach to model selection. *Journal of the American Statistical Association*, 74(365):153–160, 1979.
- Alan E Gelfand and Dipak K Dey. Bayesian model choice: asymptotics and exact calculations. *Journal of the Royal Statistical Society: Series B (Methodological)*, 56(3):501–514, 1994.
- Alexander Grigorievskiy, Neil Lawrence, and Simo Särkkä. Parallelizable sparse inverse formulation Gaussian processes (SpInGP). In *2017 IEEE 27th International Workshop on Machine Learning for Signal Processing (MLSP)*, pages 1–6. IEEE, 2017.
- Matthew J Heaton, Abhirup Datta, Andrew O Finley, Reinhard Furrer, Joseph Guinness, Rajarshi Guhaniyogi, Florian Gerber, Robert B Gramacy, Dorit Hammerling, Matthias Katzfuss, Finn Lindgren, Douglas W Nychka, Furong Sun, and Andrew Zammit-Mangion. A case study competition among methods for analyzing large spatial data. *Journal of Agricultural, Biological and Environmental Statistics*, 24(3):398–425, 2019.
- J. Hensman, A.G. Matthews, M. Filippone, and Z. Ghahramani. MCMC for variationally sparse Gaussian processes. In *Advances in Neural Information Processing Systems*, pages 1648–1656, 2015.
- James Hensman, Nicolò Fusi, and Neil D. Lawrence. Gaussian processes for big data. In *Proceedings of the Twenty-Ninth Conference on Uncertainty in Artificial Intelligence*, UAI’13, pages 282–290. AUAI Press, 2013.
- Daniel Hernández-Lobato, José M Hernández-Lobato, and Pierre Dupont. Robust multi-class gaussian process classification. In *Advances in neural information processing systems*, pages 280–288, 2011.
- Jari Kaipio and Erkki Somersalo. *Statistical and computational inverse problems*. Springer Science & Business Media, 2006.
- Hyoung-Moon Kim, Bani K Mallick, and CC Holmes. Analyzing nonstationary spatial data using piecewise Gaussian processes. *Journal of the American Statistical Association*, 100(470):653–668, 2005.
- Finn Lindgren, Håvard Rue, and Johan Lindström. An explicit link between Gaussian fields and Gaussian Markov random fields: the stochastic partial differential equation approach. *Journal of the Royal Statistical Society: Series B (Statistical Methodology)*, 73(4):423–498, 2011.
- Anne-Marie Lyne, Mark Girolami, Yves Atchadé, Heiko Strathmann, Daniel Simpson, et al. On Russian roulette estimates for Bayesian inference with doubly-intractable likelihoods. *Statistical science*, 30(4):443–467, 2015.
- Dougal Maclaurin and Ryan P Adams. Firefly monte carlo: exact mcmc with subsets of data. In *Proceedings of the 24th International Conference on Artificial Intelligence*, pages 4289–4295, 2015.
- Paul Marjoram, John Molitor, Vincent Plagnol, and Simon Tavaré. Markov chain monte carlo without likelihoods. *Proceedings of the National Academy of Sciences*, 100(26):15324–15328, 2003.

- G Mastroianni and G Monegato. Error estimates for gauss-laguerre and gauss-hermite quadrature formulas. In *Approximation and Computation: A Festschrift in Honor of Walter Gautschi*, pages 421–434. Springer, 1994.
- Georges Matheron. The intrinsic random functions and their applications. *Advances in Applied Probability*, pages 439–468, 1973.
- Alexander G de G Matthews, James Hensman, Richard Turner, and Zoubin Ghahramani. On sparse variational methods and the Kullback-Leibler divergence between stochastic processes. *Journal of Machine Learning Research*, 51: 231–239, 2016.
- Silvia Montagna and Surya T Tokdar. Computer emulation with nonstationary Gaussian processes. *SIAM/ASA Journal on Uncertainty Quantification*, 4(1):26–47, 2016.
- Karla Monterrubio-Gómez, Lassi Roininen, Sara Wade, Theodoros Damoulas, and Mark Girolami. Posterior inference for sparse hierarchical non-stationary models. *Computational Statistics & Data Analysis*, page 106954, 2020.
- Iain Murray and Matthew Graham. Pseudo-marginal slice sampling. In *Artificial Intelligence and Statistics*, pages 911–919, 2016.
- Iain Murray, Ryan Adams, and David MacKay. Elliptical slice sampling. In *Artificial Intelligence and Statistics*, pages 541–548, 2010.
- R. Neal. Monte carlo implementation of gaussian process models for bayesian regression and classification. *arXiv: Data Analysis, Statistics and Probability*, 1997.
- Hannes Nickisch and Carl Edward Rasmussen. Approximations for binary gaussian process classification. *Journal of Machine Learning Research*, 9(Oct):2035–2078, 2008.
- Christopher J Paciorek and Mark J Schervish. Spatial modelling using a new class of nonstationary covariance functions. *Environmetrics*, 17(5):483–506, 2006.
- Joaquin Quiñero-Candela and Carl Edward Rasmussen. A unifying view of sparse approximate gaussian process regression. *Journal of Machine Learning Research*, 6:1939–1959, 2005.
- Matias Quiroz, Robert Kohn, Mattias Villani, and Minh-Ngoc Tran. Speeding up mcmc by efficient data subsampling. *Journal of the American Statistical Association*, 114(526):831–843, 2019.
- Matias Quiroz, Minh-Ngoc Tran, Mattias Villani, Robert Kohn, and Khue-Dung Dang. The block-Poisson estimator for optimally tuned exact subsampling MCMC. 2020.
- Carl E Rasmussen and Zoubin Ghahramani. Infinite mixtures of Gaussian process experts. In *Advances in Neural Information Processing Systems*, pages 881–888, 2002.
- C.E. Rasmussen and C.K.I. Williams. *Gaussian processes for machine learning*. Adaptive Computation and Machine Learning Series. the MIT Press, 2006.
- Chang-han Rhee and Peter W Glynn. Unbiased estimation with square root convergence for sde models. *Operations Research*, 63(5):1026–1043, 2015.
- Gareth O Roberts and Jeffrey S Rosenthal. Examples of adaptive MCMC. *Journal of Computational and Graphical Statistics*, 18(2):349–367, 2009.
- Simone Rossi, Markus Heinonen, Edwin V. Bonilla, Zheyang Shen, and Maurizio Filippone. Sparse Gaussian processes revisited: Bayesian approaches to inducing-variable approximations, 2020.
- Matthias Seeger, Christopher KI Williams, and Neil D Lawrence. Fast forward selection to speed up sparse gaussian process regression. In *Proceedings of the Ninth International Workshop on Artificial Intelligence and Statistics*, 2003.
- E. Snelson and Z. Ghahramani. Sparse Gaussian processes using pseudo-inputs. In *Advances in Neural Information Processing Systems*, pages 1257–1264, 2006.
- Suzanne Sniekers and Aad van der Vaart. Adaptive bayesian credible sets in regression with a gaussian process prior. *Electron. J. Statist.*, 9(2):2475–2527, 2015. doi: 10.1214/15-EJS1078. URL <https://doi.org/10.1214/15-EJS1078>.
- Vassilios Stathopoulos, Veronica Zamora-Gutierrez, Kate Jones, and Mark Girolami. Bat call identification with Gaussian process multinomial probit regression and a dynamic time warping kernel. In *Artificial Intelligence and Statistics*, pages 913–921, 2014.
- Michalis Titsias. Variational learning of inducing variables in sparse gaussian processes. In *Artificial Intelligence and Statistics*, pages 567–574, 2009.
- Volker Tresp. A bayesian committee machine. *Neural computation*, 12(11):2719–2741, 2000.

- Anders Kirk Uhrenholt, Valentin Charvet, and Bjørn Sand Jensen. Probabilistic selection of inducing points in sparse Gaussian processes, 2020.
- Jarno Vanhatalo, Jaakko Riihimäki, Jouni Hartikainen, Pasi Jylänki, Ville Tolvanen, and Aki Vehtari. Bayesian modeling with Gaussian processes using the GPstuff toolbox. 2015.
- Matti Vihola, Jouni Helske, and Jordan Franks. Importance sampling type estimators based on approximate marginal markov chain monte carlo. *Scandinavian Journal of Statistics*, pages 1–38, 2020.
- Victoria Volodina and Daniel Williamson. Diagnostics-driven nonstationary emulators using kernel mixtures. *SIAM/ASA Journal on Uncertainty Quantification*, 8(1):1–26, 2020.
- Jonas Wallin and Sreekar Vadlamani. Infinite dimensional adaptive mcmc for gaussian processes. *arXiv preprint arXiv:1804.04859*, 2018.
- Yue Wu, José Miguel Hernández-Lobato, and Zoubin Ghahramani. Gaussian process volatility model. In *Advances in Neural Information Processing Systems*, pages 1044–1052, 2014.
- Xiaoyu Xiong, Václav Šmídl, and Maurizio Filippone. Adaptive multiple importance sampling for Gaussian processes. *Journal of Statistical Computation and Simulation*, 87(8):1644–1665, 2017.
- Yaming Yu and Xiao-Li Meng. To center or not to center: That is not the question—an ancillarity–sufficiency interweaving strategy (asis) for boosting mcmc efficiency. *Journal of Computational and Graphical Statistics*, 20(3): 531–570, 2011.

Appendices

A Derivations

A.1 Optimal variational posterior

We seek the variational posterior distribution which minimizes the Kullback-Leibler (KL) divergence between the approximate and true posterior,

$$\begin{aligned}
 & \text{KL}(q(z, \tilde{z}, \mathbf{u}, \tilde{\mathbf{u}}, \boldsymbol{\theta}) \| \pi(z, \tilde{z}, \mathbf{u}, \tilde{\mathbf{u}}, \boldsymbol{\theta} \mid \mathbf{y}, X, \tilde{X})) \\
 &= -\mathbb{E}_q \left[\log \left(\frac{N(\mathbf{y} \mid z, \sigma_\varepsilon^2 I) \pi(z \mid \tilde{z}, \mathbf{u}, \tilde{\mathbf{u}}, \boldsymbol{\theta}) \pi(\tilde{z} \mid \tilde{\mathbf{u}}, \boldsymbol{\theta}) \pi(\mathbf{u} \mid \tilde{\mathbf{u}}, \boldsymbol{\theta}) \pi(\tilde{\mathbf{u}} \mid \boldsymbol{\theta}) \pi(\boldsymbol{\theta})}{p(\mathbf{y} \mid X) \pi(z \mid \tilde{z}, \mathbf{u}, \tilde{\mathbf{u}}, \boldsymbol{\theta}) \pi(\mathbf{u} \mid \tilde{\mathbf{u}}, \boldsymbol{\theta}) q(\tilde{z}, \tilde{\mathbf{u}}, \boldsymbol{\theta})} \right) \right] \\
 &= -\mathbb{E}_q \left[\log \left(\frac{N(\mathbf{y} \mid z, \sigma_\varepsilon^2 I) \pi(\tilde{z} \mid \tilde{\mathbf{u}}, \boldsymbol{\theta}) \pi(\tilde{\mathbf{u}} \mid \boldsymbol{\theta}) \pi(\boldsymbol{\theta})}{q(\tilde{z}, \tilde{\mathbf{u}}, \boldsymbol{\theta})} \right) \right] + \log(p(\mathbf{y} \mid X)) \\
 &= -\mathbb{E}_{q(\tilde{z}, \tilde{\mathbf{u}}, \boldsymbol{\theta})} \left[\log \left(\frac{\exp(\mathbb{E}_{\pi(z, \mathbf{u} \mid \tilde{z}, \tilde{\mathbf{u}}, \boldsymbol{\theta})} [\log(N(\mathbf{y} \mid z, \sigma_\varepsilon^2 I))]) \pi(\tilde{z} \mid \tilde{\mathbf{u}}, \boldsymbol{\theta}) \pi(\tilde{\mathbf{u}} \mid \boldsymbol{\theta}) \pi(\boldsymbol{\theta})}{q(\tilde{z}, \tilde{\mathbf{u}}, \boldsymbol{\theta})} \right) \right] \\
 &\quad + \log(p(\mathbf{y} \mid X)).
 \end{aligned}$$

Thus, minimisation reveals that the optimal variational posterior is

$$q(\tilde{z}, \tilde{\mathbf{u}}, \boldsymbol{\theta}) \propto \exp \left(\sum_{n=1}^N \mathbb{E}_{(z_n, u_n)} [\log(N(y_n \mid z_n, \sigma_\varepsilon^2))] \right) \pi(\tilde{z} \mid \tilde{\mathbf{u}}, \boldsymbol{\theta}) \pi(\tilde{\mathbf{u}} \mid \boldsymbol{\theta}) \pi(\boldsymbol{\theta}). \quad (19)$$

A.2 Marginal variational posterior

Consider the optimal variational posterior in eq. (19). Our goal is to marginalise \tilde{z} to obtain $q(\tilde{\mathbf{u}}, \boldsymbol{\theta})$ and consequently derive the conditional variational posterior $q(\tilde{z} \mid \tilde{\mathbf{u}}, \boldsymbol{\theta})$. First, let us rewrite eq. (19) as:

$$q(\tilde{z}, \tilde{\mathbf{u}}, \boldsymbol{\theta}) \propto \exp \left(\sum_{n=1}^N \mathbb{E}_{u_n} [l(y_n \mid u_n, \tilde{z}, \boldsymbol{\theta})] \right) \pi(\tilde{z} \mid \tilde{\mathbf{u}}, \boldsymbol{\theta}) \pi(\tilde{\mathbf{u}} \mid \boldsymbol{\theta}) \pi(\boldsymbol{\theta}),$$

where

$$\begin{aligned}
 l(y_n \mid u_n, \tilde{z}, \boldsymbol{\theta}) &= \mathbb{E}_{z_n} [\log(N(y_n \mid z_n, \sigma_\varepsilon^2)) \mid u_n] \\
 &= -\frac{1}{2} \log(2\pi\sigma_\varepsilon^2) - \frac{1}{2\sigma_\varepsilon^2} [(y_n - \mathbb{E}_{z_n} [z_n \mid u_n])^2 + V_{z_n}(z_n \mid u_n)] \\
 &= -\frac{1}{2} \log(2\pi\sigma_\varepsilon^2) - \frac{1}{2\sigma_\varepsilon^2} [(y_n - \mathbf{C}_{z_n, \tilde{z}}^{\text{NS}} (\mathbf{C}_{\tilde{z}, \tilde{z}}^{\text{NS}})^{-1} \tilde{z})^2 + \tau_z^2 - \mathbf{C}_{z_n, \tilde{z}}^{\text{NS}} (\mathbf{C}_{\tilde{z}, \tilde{z}}^{\text{NS}})^{-1} \mathbf{C}_{\tilde{z}, z_n}^{\text{NS}}].
 \end{aligned}$$

Then, by expanding the terms inside the exponent and defining

$$\boldsymbol{\beta}_n = \mathbb{E}_{u_n} [\mathbf{C}_{z_n, \tilde{z}}^{\text{NS}}], \quad \mathbf{P}_n = \mathbb{E}_{u_n} [\mathbf{C}_{\tilde{z}, z_n}^{\text{NS}} \mathbf{C}_{z_n, \tilde{z}}^{\text{NS}}], \quad \text{and} \quad \alpha_n = \mathbb{E}_{u_n} [\mathbf{C}_{z_n, \tilde{z}}^{\text{NS}} (\mathbf{C}_{\tilde{z}, \tilde{z}}^{\text{NS}})^{-1} \mathbf{C}_{\tilde{z}, z_n}^{\text{NS}}]$$

we obtain:

$$\begin{aligned}
 q(\tilde{z}, \tilde{\mathbf{u}}, \boldsymbol{\theta}) &\propto \left(\frac{\sigma_\varepsilon^{-2}}{2\pi} \right)^{\frac{N}{2}} \pi(\tilde{z} \mid \tilde{\mathbf{u}}, \boldsymbol{\theta}) \pi(\tilde{\mathbf{u}} \mid \boldsymbol{\theta}) \pi(\boldsymbol{\theta}) \times \\
 &\exp \left(-\frac{1}{2\sigma_\varepsilon^2} \sum_{n=1}^N y_n^2 - 2y_n \boldsymbol{\beta}_n (\mathbf{C}_{\tilde{z}, \tilde{z}}^{\text{NS}})^{-1} \tilde{z} + \cancel{\boldsymbol{\beta}_n (\mathbf{C}_{\tilde{z}, \tilde{z}}^{\text{NS}})^{-1} \tilde{z} (\boldsymbol{\beta}_n (\mathbf{C}_{\tilde{z}, \tilde{z}}^{\text{NS}})^{-1} \tilde{z})^T} + \tau_z^2 - \alpha_n + \right. \\
 &\quad \left. \tilde{z}^T (\mathbf{C}_{\tilde{z}, \tilde{z}}^{\text{NS}})^{-1} \mathbf{P}_n (\mathbf{C}_{\tilde{z}, \tilde{z}}^{\text{NS}})^{-1} \tilde{z} - \cancel{\tilde{z}^T (\mathbf{C}_{\tilde{z}, \tilde{z}}^{\text{NS}})^{-1} (\boldsymbol{\beta}_n^T \boldsymbol{\beta}_n) (\mathbf{C}_{\tilde{z}, \tilde{z}}^{\text{NS}})^{-1} \tilde{z}} \right), \quad (20)
 \end{aligned}$$

Now, let us collect the terms that do not depend on \tilde{z} in

$$\Xi := \left(\frac{\sigma_\varepsilon^{-2}}{2\pi} \right)^{\frac{N}{2}} \pi(\tilde{\mathbf{u}} \mid \boldsymbol{\theta}) \pi(\boldsymbol{\theta}) \exp \left(-\frac{1}{2\sigma_\varepsilon^2} \sum_{n=1}^N y_n^2 + \tau_z^2 - \alpha_n \right),$$

and re-write Eq. (20) as

$$\begin{aligned}
 q(\tilde{\mathbf{z}}, \tilde{\mathbf{u}}, \boldsymbol{\theta}) &\propto \Xi \exp \left(-\frac{1}{2\sigma_\epsilon^2} \sum_{n=1}^N -2y_n \beta_n (C_{\tilde{\mathbf{z}}, \tilde{\mathbf{z}}}^{\text{NS}})^{-1} \tilde{\mathbf{z}} + \tilde{\mathbf{z}}^T (C_{\tilde{\mathbf{z}}, \tilde{\mathbf{z}}}^{\text{NS}})^{-1} \mathbf{P}_n (C_{\tilde{\mathbf{z}}, \tilde{\mathbf{z}}}^{\text{NS}})^{-1} \tilde{\mathbf{z}} \right) \pi(\tilde{\mathbf{z}} | \tilde{\mathbf{u}}, \boldsymbol{\theta}) \\
 &\propto \Xi \exp \left(-\frac{1}{2\sigma_\epsilon^2} \sum_{n=1}^N -2y_n \beta_n (C_{\tilde{\mathbf{z}}, \tilde{\mathbf{z}}}^{\text{NS}})^{-1} \tilde{\mathbf{z}} + \tilde{\mathbf{z}}^T (C_{\tilde{\mathbf{z}}, \tilde{\mathbf{z}}}^{\text{NS}})^{-1} \mathbf{P}_n (C_{\tilde{\mathbf{z}}, \tilde{\mathbf{z}}}^{\text{NS}})^{-1} \tilde{\mathbf{z}} \right) \text{N}(\tilde{\mathbf{z}} | 0, C_{\tilde{\mathbf{z}}, \tilde{\mathbf{z}}}^{\text{NS}}) \\
 &\propto \Xi \exp \left(\sigma_\epsilon^{-2} \mathbf{y}^T \mathbf{B} (C_{\tilde{\mathbf{z}}, \tilde{\mathbf{z}}}^{\text{NS}})^{-1} \tilde{\mathbf{z}} - \frac{1}{2} \tilde{\mathbf{z}}^T (C_{\tilde{\mathbf{z}}, \tilde{\mathbf{z}}}^{\text{NS}})^{-1} \sigma_\epsilon^{-2} \mathbf{P} (C_{\tilde{\mathbf{z}}, \tilde{\mathbf{z}}}^{\text{NS}})^{-1} \tilde{\mathbf{z}} \right) \text{N}(\tilde{\mathbf{z}} | 0, C_{\tilde{\mathbf{z}}, \tilde{\mathbf{z}}}^{\text{NS}}),
 \end{aligned}$$

where $\mathbf{P} = \sum_{n=1}^N \mathbf{P}_n$ and \mathbf{B} an $(N \times M)$ matrix with rows β_n .

The marginal variational posterior $q(\tilde{\mathbf{u}}, \boldsymbol{\theta}) = \int q(\tilde{\mathbf{z}}, \tilde{\mathbf{u}}, \boldsymbol{\theta}) d\tilde{\mathbf{z}}$ is therefore:

$$\begin{aligned}
 q(\tilde{\mathbf{u}}, \boldsymbol{\theta}) &\propto \int \Xi \exp \left(\sigma_\epsilon^{-2} \mathbf{y}^T \mathbf{B} (C_{\tilde{\mathbf{z}}, \tilde{\mathbf{z}}}^{\text{NS}})^{-1} \tilde{\mathbf{z}} - \frac{1}{2} \tilde{\mathbf{z}}^T (C_{\tilde{\mathbf{z}}, \tilde{\mathbf{z}}}^{\text{NS}})^{-1} \sigma_\epsilon^{-2} \mathbf{P} (C_{\tilde{\mathbf{z}}, \tilde{\mathbf{z}}}^{\text{NS}})^{-1} \tilde{\mathbf{z}} \right) \text{N}(\tilde{\mathbf{z}} | 0, C_{\tilde{\mathbf{z}}, \tilde{\mathbf{z}}}^{\text{NS}}) d\tilde{\mathbf{z}} \\
 &\propto \Xi |C_{\tilde{\mathbf{z}}, \tilde{\mathbf{z}}}^{\text{NS}}|^{-\frac{1}{2}} \int \exp \left(\sigma_\epsilon^{-2} \mathbf{y}^T \mathbf{B} (C_{\tilde{\mathbf{z}}, \tilde{\mathbf{z}}}^{\text{NS}})^{-1} \tilde{\mathbf{z}} - \frac{1}{2} \tilde{\mathbf{z}}^T (C_{\tilde{\mathbf{z}}, \tilde{\mathbf{z}}}^{\text{NS}})^{-1} \sigma_\epsilon^{-2} \mathbf{P} (C_{\tilde{\mathbf{z}}, \tilde{\mathbf{z}}}^{\text{NS}})^{-1} \tilde{\mathbf{z}} \right. \\
 &\quad \left. - \frac{1}{2} \tilde{\mathbf{z}}^T (C_{\tilde{\mathbf{z}}, \tilde{\mathbf{z}}}^{\text{NS}})^{-1} \tilde{\mathbf{z}} \right) d\tilde{\mathbf{z}} \\
 &\propto \Xi |C_{\tilde{\mathbf{z}}, \tilde{\mathbf{z}}}^{\text{NS}}|^{-\frac{1}{2}} \int \exp \left(\sigma_\epsilon^{-2} \mathbf{y}^T \mathbf{B} (C_{\tilde{\mathbf{z}}, \tilde{\mathbf{z}}}^{\text{NS}})^{-1} \tilde{\mathbf{z}} - \frac{1}{2} \tilde{\mathbf{z}}^T [(C_{\tilde{\mathbf{z}}, \tilde{\mathbf{z}}}^{\text{NS}})^{-1} \sigma_\epsilon^{-2} \mathbf{P} (C_{\tilde{\mathbf{z}}, \tilde{\mathbf{z}}}^{\text{NS}})^{-1} + C_{\tilde{\mathbf{z}}, \tilde{\mathbf{z}}}^{\text{NS}}] \tilde{\mathbf{z}} \right) d\tilde{\mathbf{z}}.
 \end{aligned} \tag{21}$$

We now notice that the terms inside the integral resemble the kernel of Gaussian with mean and variance

$$\begin{aligned}
 \hat{\boldsymbol{\mu}}_{\tilde{\mathbf{z}}} &= \sigma_\epsilon^{-2} C_{\tilde{\mathbf{z}}, \tilde{\mathbf{z}}}^{\text{NS}} (\sigma_\epsilon^{-2} \mathbf{P} + C_{\tilde{\mathbf{z}}, \tilde{\mathbf{z}}}^{\text{NS}})^{-1} \mathbf{B}^T \mathbf{y}, \\
 \hat{\boldsymbol{\Sigma}}_{\tilde{\mathbf{z}}} &= ((C_{\tilde{\mathbf{z}}, \tilde{\mathbf{z}}}^{\text{NS}})^{-1} \sigma_\epsilon^{-2} \mathbf{P} (C_{\tilde{\mathbf{z}}, \tilde{\mathbf{z}}}^{\text{NS}})^{-1} + C_{\tilde{\mathbf{z}}, \tilde{\mathbf{z}}}^{\text{NS}})^{-1} \\
 &= C_{\tilde{\mathbf{z}}, \tilde{\mathbf{z}}}^{\text{NS}} (\sigma_\epsilon^{-2} \mathbf{P} + C_{\tilde{\mathbf{z}}, \tilde{\mathbf{z}}}^{\text{NS}})^{-1} C_{\tilde{\mathbf{z}}, \tilde{\mathbf{z}}}^{\text{NS}}.
 \end{aligned}$$

Thus, by completing the square, we re-write Eq. (21) as

$$\begin{aligned}
 q(\tilde{\mathbf{u}}, \boldsymbol{\theta}) &\propto \Xi |C_{\tilde{\mathbf{z}}, \tilde{\mathbf{z}}}^{\text{NS}}|^{\frac{1}{2}} |\sigma_\epsilon^{-2} \mathbf{P} + C_{\tilde{\mathbf{z}}, \tilde{\mathbf{z}}}^{\text{NS}}|^{\frac{1}{2}} \exp \left(\frac{\sigma_\epsilon^{-4}}{2} (\mathbf{y}^T \mathbf{B} (\sigma_\epsilon^{-2} \mathbf{P} + C_{\tilde{\mathbf{z}}, \tilde{\mathbf{z}}}^{\text{NS}})^{-1} \mathbf{B}^T \mathbf{y}) \right) \\
 &\quad \times \int \text{N}(\tilde{\mathbf{z}} | \hat{\boldsymbol{\mu}}_{\tilde{\mathbf{z}}}, \hat{\boldsymbol{\Sigma}}_{\tilde{\mathbf{z}}}) d\tilde{\mathbf{z}},
 \end{aligned}$$

where by plugging the values of Ξ and re-arranging terms, we obtain

$$\begin{aligned}
 q(\tilde{\mathbf{u}}, \boldsymbol{\theta}) &\propto \sigma_\epsilon^{-N} \pi(\tilde{\mathbf{u}} | \boldsymbol{\theta}) \pi(\boldsymbol{\theta}) \exp \left(\frac{1}{2\sigma_\epsilon^4} \mathbf{y}^T \mathbf{B} (C_{\tilde{\mathbf{z}}, \tilde{\mathbf{z}}}^{\text{NS}} + \sigma_\epsilon^{-2} \mathbf{P})^{-1} \mathbf{B}^T \mathbf{y} \right) \\
 &\quad |C_{\tilde{\mathbf{z}}, \tilde{\mathbf{z}}}^{\text{NS}} + \sigma_\epsilon^{-2} \mathbf{P}|^{-\frac{1}{2}} |C_{\tilde{\mathbf{z}}, \tilde{\mathbf{z}}}^{\text{NS}}|^{\frac{1}{2}} \exp \left(-\frac{1}{2\sigma_\epsilon^2} \sum_{n=1}^N (y_n^2 + \tau_z^2) + \frac{1}{2\sigma_\epsilon^2} \sum_{n=1}^N \alpha_n \right),
 \end{aligned}$$

with

$$\begin{aligned}
 \sum_{n=1}^N \alpha_n &= \sum_{n=1}^N \mathbb{E}_{u_n} [C_{z_n, \tilde{\mathbf{z}}}^{\text{NS}} (C_{\tilde{\mathbf{z}}, \tilde{\mathbf{z}}}^{\text{NS}})^{-1} C_{\tilde{\mathbf{z}}, z_n}^{\text{NS}}] \\
 &= \sum_{i,j=1}^M (C_{\tilde{\mathbf{z}}, \tilde{\mathbf{z}}}^{\text{NS}})^{-1}_{ij} \sum_{n=1}^N \mathbb{E}_{u_n} [C_{\tilde{z}_i, z_n}^{\text{NS}} C_{z_n, \tilde{z}_j}^{\text{NS}}] \\
 &= \sum_{i,j=1}^M (C_{\tilde{\mathbf{z}}, \tilde{\mathbf{z}}}^{\text{NS}})^{-1}_{ij} \mathbf{P}_{ij} \\
 &= \sum_{i,j=1}^M (C_{\tilde{\mathbf{z}}, \tilde{\mathbf{z}}}^{\text{NS}})^{-1} \odot \mathbf{P}_{ij}.
 \end{aligned}$$

The conditional variational posterior is Gaussian with mean $\hat{\boldsymbol{\mu}}_{\tilde{\mathbf{z}}}$ and variance $\hat{\Sigma}_{\tilde{\mathbf{z}}}$, such that

$$q(\tilde{\mathbf{z}} \mid \tilde{\mathbf{u}}, \boldsymbol{\theta}) = \mathcal{N}\left(\sigma_{\varepsilon}^{-2} C_{\tilde{\mathbf{z}}, \tilde{\mathbf{z}}}^{\text{NS}} (\sigma_{\varepsilon}^{-2} \mathbf{P} + C_{\tilde{\mathbf{z}}, \tilde{\mathbf{z}}}^{\text{NS}})^{-1} \mathbf{B}^T \mathbf{y}, \sigma_{\varepsilon}^{-2} C_{\tilde{\mathbf{z}}, \tilde{\mathbf{z}}}^{\text{NS}} (\sigma_{\varepsilon}^{-2} \mathbf{P} + C_{\tilde{\mathbf{z}}, \tilde{\mathbf{z}}}^{\text{NS}})^{-1} \mathbf{B}^T \mathbf{y}\right).$$

A.3 Derivative

To compute the difference estimator for the two-level GP model, we need to calculate the first-order Taylor expansion $\nu_n(u_n)$, which requires the derivative

$$\frac{d}{du_n} l(y_n \mid u_n, \tilde{\mathbf{z}}, \boldsymbol{\theta}) = \frac{1}{\sigma_{\varepsilon}^2} \left[(y_n - C_{z_n, \tilde{\mathbf{z}}}^{\text{NS}} (C_{\tilde{\mathbf{z}}, \tilde{\mathbf{z}}}^{\text{NS}})^{-1} \tilde{\mathbf{z}}) \frac{\partial C_{z_n, \tilde{\mathbf{z}}}^{\text{NS}}}{\partial u_n} (C_{\tilde{\mathbf{z}}, \tilde{\mathbf{z}}}^{\text{NS}})^{-1} \tilde{\mathbf{z}} + \frac{\partial C_{z_n, \tilde{\mathbf{z}}}^{\text{NS}}}{\partial u_n} (C_{\tilde{\mathbf{z}}, \tilde{\mathbf{z}}}^{\text{NS}})^{-1} C_{\tilde{\mathbf{z}}, z_n}^{\text{NS}} \right]$$

where the m th entry of $\frac{\partial C_{z_n, \tilde{\mathbf{z}}}^{\text{NS}}}{\partial u_n}$ is given by $\frac{\partial C_{z_n, z_m}^{\text{NS}}}{\partial u_n}$ with C_{z_n, z_m}^{NS} obtained through Eq. (12). In this case, the derivative for the non-stationary isotropic SE kernel is:

$$\begin{aligned} \frac{\partial C_{z_n, \tilde{\mathbf{z}}}^{\text{NS}}}{\partial u_n} &= \ell_n \left(\frac{\ell_n}{2\tilde{\ell}_m} + \frac{\tilde{\ell}_m}{2\ell_n} \right)^{-\frac{D}{2}} \exp\left(-\frac{\|\mathbf{x}_n - \tilde{\mathbf{x}}_m\|^2}{\ell_n^2 + \tilde{\ell}_m^2}\right) \times \\ &\quad \left[\left(\frac{\ell_n}{\tilde{\ell}_m} + \frac{\tilde{\ell}_m}{\ell_n} \right)^{-1} \left(\frac{-D}{2\tilde{\ell}_m} + \frac{D\tilde{\ell}_m}{2\ell_n^2} \right) + \frac{2\ell_n}{(\ell_n^2 + \tilde{\ell}_m^2)^2} \|\mathbf{x}_n - \tilde{\mathbf{x}}_m\|^2 \right]. \end{aligned}$$

A.4 Control variates

Note that computing $l(y_n \mid u_n, \tilde{\mathbf{z}}, \boldsymbol{\theta})$ is $\mathcal{O}(NM^2)$. Thus, computing the control variates is $\mathcal{O}(NM^2)$ and the cost of block-Poisson estimator is $\mathcal{O}(NM^2 + \kappa BM^2)$. We can reduce this to $\mathcal{O}(NM + \kappa BM^2)$ by defining:

$$l(y_n \mid u_n, \tilde{\mathbf{z}}, \boldsymbol{\theta}) = l_1(y_n \mid u_n, \tilde{\mathbf{z}}, \boldsymbol{\theta}) + l_2(y_n \mid u_n, \tilde{\mathbf{z}}, \boldsymbol{\theta}),$$

where

$$\begin{aligned} l_1(y_n \mid u_n, \tilde{\mathbf{z}}, \boldsymbol{\theta}) &= -\frac{1}{2} \log(2\pi\sigma_{\varepsilon}^2) - \frac{1}{2\sigma_{\varepsilon}^2} [(y_n - C_{z_n, \tilde{\mathbf{z}}}^{\text{NS}} (C_{\tilde{\mathbf{z}}, \tilde{\mathbf{z}}}^{\text{NS}})^{-1} \tilde{\mathbf{z}})^2], \\ l_2(y_n \mid u_n, \boldsymbol{\theta}) &= -\frac{1}{2\sigma_{\varepsilon}^2} [\tau_z^2 - C_{z_n, \tilde{\mathbf{z}}}^{\text{NS}} (C_{\tilde{\mathbf{z}}, \tilde{\mathbf{z}}}^{\text{NS}})^{-1} C_{\tilde{\mathbf{z}}, z_n}^{\text{NS}}]. \end{aligned}$$

and defining the control variates as the expectation of $\nu_n(u_n)$, which is a first order Talyor expansion of $l_1(y_n \mid u_n, \tilde{\mathbf{z}}, \boldsymbol{\theta})$ around $\mathbb{E}[u_n]$. Thus, the control variates are:

$$\bar{\nu}_n = l_1(y_n \mid \mathbb{E}[u_n], \tilde{\mathbf{z}}, \boldsymbol{\theta}),$$

which is $\mathcal{O}(NM)$. This would only be beneficial if $\kappa B < N$.

A.5 Inducing points

As alternative, we propose to use the pilot MCMC to select the number of inducing points by optimizing a measure that combines both accuracy and computational cost. To measure accuracy, we consider the log-pseudo marginal likelihood [LPML, Geisser and Eddy, 1979]:

$$\begin{aligned} \text{LPML} &= \sum_{n=1}^N \log(\text{CPO}_n), \\ \text{CPO}_n &\approx \left(\frac{1}{S} \sum_{s=1}^S \left[p(y_n \mid \mathbb{E}[z_n \mid \tilde{\boldsymbol{\xi}}^s, \boldsymbol{\phi}^s], \boldsymbol{\rho}^s) \right]^{-1} \right)^{-1}, \end{aligned}$$

where the conditional predictive ordinate (CPO) is approximated by the harmonic mean [Gelfand and Dey, 1994] and to reduce computational cost, we plug-in the expectation of z_n . The number of inducing points can then be selected to maximize LMPL/CT, to explicitly account for the desire to maximize the marginal likelihood and also minimize computational cost.

A.6 Approximate MCMC for two-level GP regression

We discuss the algorithm employ to sample from the whitened marginal approximated posterior. The sampler is detailed for the case when a squared exponential covariance function is employed for both the stationary and non-stationary processes. In addition, to improve parameter identifiability, we make use of the empirical prior approach discussed in Monterrubio-Gómez et al. [2020] to fix the magnitude and mean of the length-scale processes. Furthermore, we standarize the observations, \mathbf{y} , to have zero mean and unit variance, such that fixing $\tau_z^2 = 1$ is an appropriate assumption. We let $\boldsymbol{\lambda} = (\lambda_1 \dots \lambda_D)$ denote the length-scale parameters for the second level stationary GP prior.

The proposed algorithm uses a MwG scheme, where the whitened spatially varying parameters are sampled employing elliptical slice sampling [ELLSS, Murray et al., 2010] and the remaining parameters are drawn with an adaptive random-walk MH procedure [Roberts and Rosenthal, 2009, Section 3]. With exception of the noise variance, the sampling mechanism requires to approximate the relevant quantities in Eq. (15) when iterating over $(\tilde{\zeta}, \boldsymbol{\lambda})$. For efficiency, the positions and associated weights required in the quadrature schemes can be precomputed, prior to running the MCMC, and passed to the samplers. The R package fastGHQuad [Blocker, 2018] is employed to compute the weights and nodes.

A.7 Exact MCMC for two-level GP regression

We present details on how to sample from the whitened approximate posterior distribution for a variationally sparse 2-level GP model with an isotropic assumption for the non-stationary kernel. Again, here, we fix some of the parameters employing empirical priors. For the optimal tuning parameters we follow the approach described in Section 3.3, resulting in a slight modification of Algorithm 2, where we add an extra step after generating the pilot MCMC samples. This extra step aims to draw S samples from $\tilde{\mathbf{z}} \mid \tilde{\mathbf{u}}, \boldsymbol{\theta}$. For the pilot MCMC we utilise the already implemented algorithm based on Gauss-Hermite quadrature with $J = 10$.

In a similar fashion to Algorithm 1, the proposed scheme uses a MwG sampler to iterate over $(\tilde{\xi}, \tilde{\zeta}, \sigma_\varepsilon^2, \boldsymbol{\lambda})$. The noise variance σ_ε^2 and second level length-scale $\boldsymbol{\lambda}$, are sampled with adaptive random-walk MH steps [Roberts and Rosenthal, 2009, Section 3]. For the whitened spatially varying length-scale, we employ ELLSS [Murray et al., 2010], and for the non-stationary function $\tilde{\mathbf{z}}$, we use an independent MH step with a Gaussian proposal that approximates the true variational conditional posterior; more precisely, the proposal is:

$$\mathcal{N} \left(\sigma_\varepsilon^{-2} C_{\tilde{\mathbf{z}}, \tilde{\mathbf{z}}}^{\text{NS}} \left(C_{\tilde{\mathbf{z}}, \tilde{\mathbf{z}}}^{\text{NS}} + \sigma_\varepsilon^{-2} \hat{\mathbf{P}} \right)^{-1} \hat{\mathbf{B}}^T \mathbf{y}, C_{\tilde{\mathbf{z}}, \tilde{\mathbf{z}}}^{\text{NS}} \left(C_{\tilde{\mathbf{z}}, \tilde{\mathbf{z}}}^{\text{NS}} + \sigma_\varepsilon^{-2} \hat{\mathbf{P}} \right)^{-1} C_{\tilde{\mathbf{z}}, \tilde{\mathbf{z}}}^{\text{NS}} \right),$$

with $\hat{\mathbf{B}}$ an $N \times M$ matrix with rows $\hat{\beta}_n = [C_{z_n, \tilde{\mathbf{z}}}^{\text{NS}}]_{\mu_{\ell_n}}$ and $\hat{\mathbf{P}} = \sum_{n=1}^N \hat{\mathbf{P}}_n$, with $\hat{\mathbf{P}}_n = [C_{\tilde{\mathbf{z}}, z_n}^{\text{NS}} C_{z_n, \tilde{\mathbf{z}}}^{\text{NS}}]_{\mu_{\ell_n}}$, where we use $\mu_{\ell_n} = \exp(c_n + w_n^2/2)$ to evaluate the expressions in square brackets with

$$\begin{aligned} c_n &= \mu_u + C_{u_n, \tilde{\mathbf{u}}}^S (C_{\tilde{\mathbf{u}}, \tilde{\mathbf{u}}}^S)^{-1} (L(\boldsymbol{\varphi}) \tilde{\zeta} + \mu_u), \\ w_n^2 &= \tau_u^2 - C_{u_n, \tilde{\mathbf{u}}}^S (C_{\tilde{\mathbf{u}}, \tilde{\mathbf{u}}}^S)^{-1} C_{\tilde{\mathbf{u}}, u_n}^S. \end{aligned}$$

The computational complexity of the algorithm is $\mathcal{O}((\sum_{k=1}^{\kappa} \mathcal{H}_k) B M^2 + M^3 + N M^2)$. We emphasise that for all the parameter updates, we can compute the difference estimator $\hat{d}_{\alpha_b, h, k}$ for all h and k , in parallel. While our current implementation does not make use of parallel computing, this can be adapted to vectorise some of the operations; for instance, $c_n, w_n, l(y_n \mid u_n, \sigma_\varepsilon^2, \boldsymbol{\lambda}, \tilde{\xi}, \tilde{\zeta})$, and $l'(y_n \mid c_n, \sigma_\varepsilon^2, \boldsymbol{\lambda}, \tilde{\xi}, \tilde{\zeta})$ can be easily vectorised.

B Simulation study

B.1 1-dimensional dataset

B.1.1 Optimal tuning parameters and CT*

To find the optimal number of Poisson estimators, κ , for a fixed value of $B = 30$, we utilise a slight modification of Algorithm 2, where we add an extra step after generating $S = 1000$ MCMC samples from a pilot run which employs a GH quadrature approximation. This extra step aims to draw samples from $\tilde{\mathbf{z}} \mid \tilde{\mathbf{u}}, \boldsymbol{\theta}$, which will be employed to compute the difference estimator. As discussed in Section 3.3, a conservative approach is to set the value of γ at its maximum across different subsamples to do a grid search of κ over $\{4, 5, \dots, 100\}$. Once the optimal κ value is computed, the lower bound is set to $a = \bar{d} - \kappa$. The results of this approach are shown in Table 1 for the different number of inducing points studied. According to this, we employ $B = 30$ subsamples and we set the optimal $\kappa = 4$

for all $M = 30, 45$, and 60 . In addition, this table also shows CT^* , as well as our proposed measure to select the number of inducing points introduced in Section A.5. According to $LPLM/CT^*$, the maximum value is attained with $M = 60$.

	γ_{\max}	κ	\bar{d} (e-05)	CT^* (e+06)	LPLM	LPLM/ CT^*
$M = 30$	2.1755	4	-2.72	1.12	-7,088.8	-0.00634
$M = 45$	0.5352	4	6.13	2.49	-9,145.5	-0.00367
$M = 60$	1.8759	4	172	4.61	-16,874.7	-0.00366

Table 1: Optimal tuning parameters values and CT^* values for $M = 30, 45$, and 60 .

Finally, Figure 6 confirms the normality assumption required by the difference estimate to find the optimal tuning parameters using Algorithm 2.

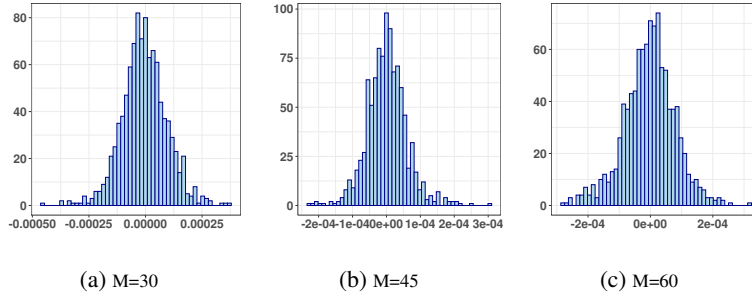


Figure 6: Histograms of \hat{d}_B with $B = 30$ for different numbers of inducing points ($M = 30, 45, 60$).

B.1.2 Posterior inference and predictions

		Avg. time (min)	Avg. evaluations
Full MCMC		15.13	9.71
$M = 30$	$J = 4$	1.41	9.53
	$J = 5$	1.69	9.53
	$J = 8$	2.53	9.53
	$J = 10$	3.06	9.53
	$J = 15$	4.34	9.53
	S-BP-PM	0.48	11.32
$M = 45$	$J = 4$	1.90	8.84
	$J = 5$	2.42	9.35
	$J = 8$	3.77	9.34
	$J = 10$	4.82	9.91
	$J = 15$	6.21	8.73
	S-BP-PM	0.73	11.98
$M = 60$	$J = 4$	2.68	9.42
	$J = 5$	3.62	9.79
	$J = 8$	5.25	9.02
	$J = 10$	6.56	9.18
	$J = 15$	9.44	9.13
	S-BP-PM	1.17	12.08

Table 2: Average time (in minutes) and likelihood evaluations required in the MCMC scheme. The average time required for 100 iterations is reported in minutes. The average number of likelihood evaluations in the elliptical slice sampler per iteration is reported.

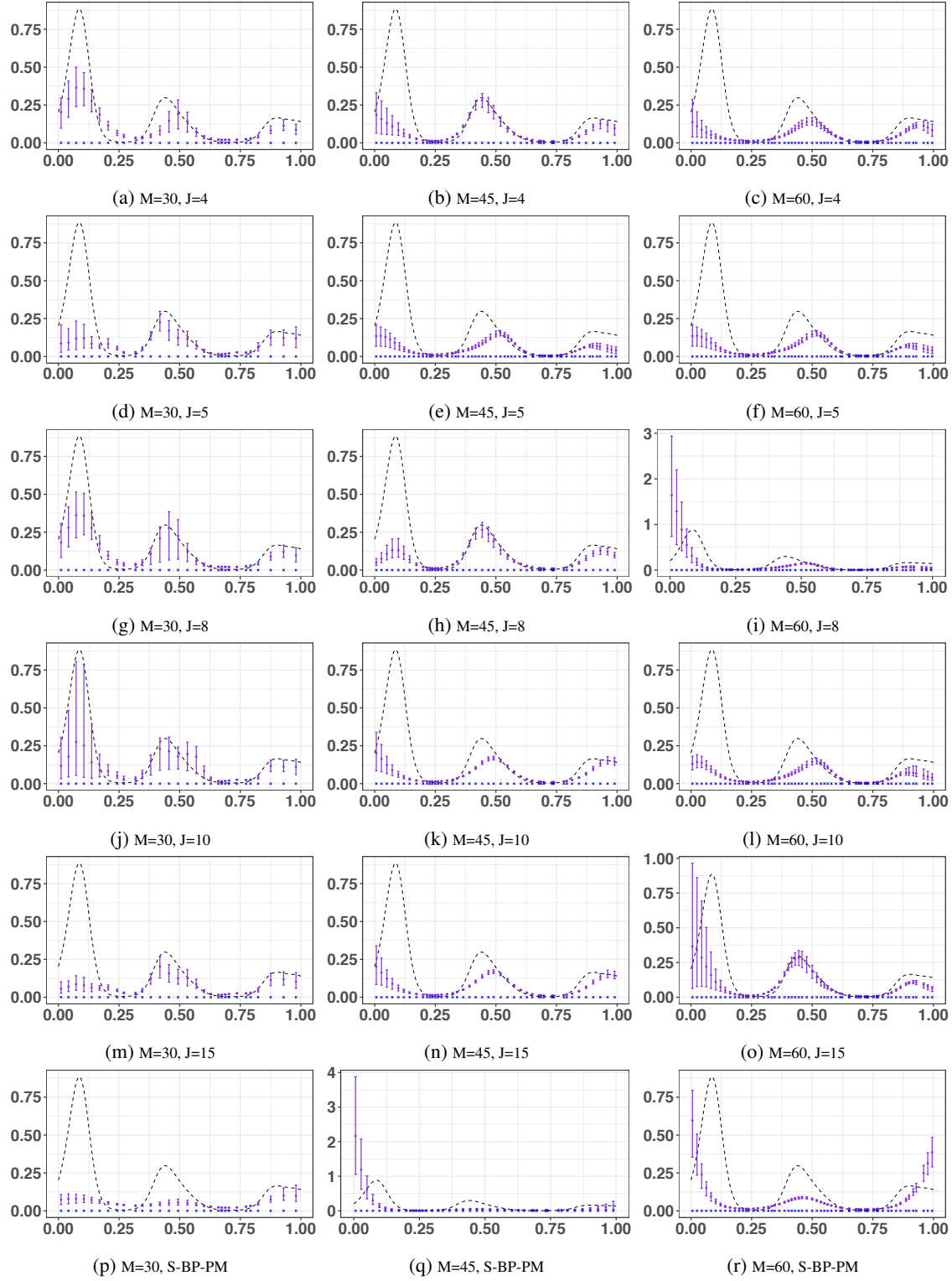


Figure 7: Posterior estimates for spatially varying parameter $\ell(\cdot)$. The dashed line denotes the true process. Purple dots and bars show posterior estimates at the inducing locations with 95% HPD credible intervals.

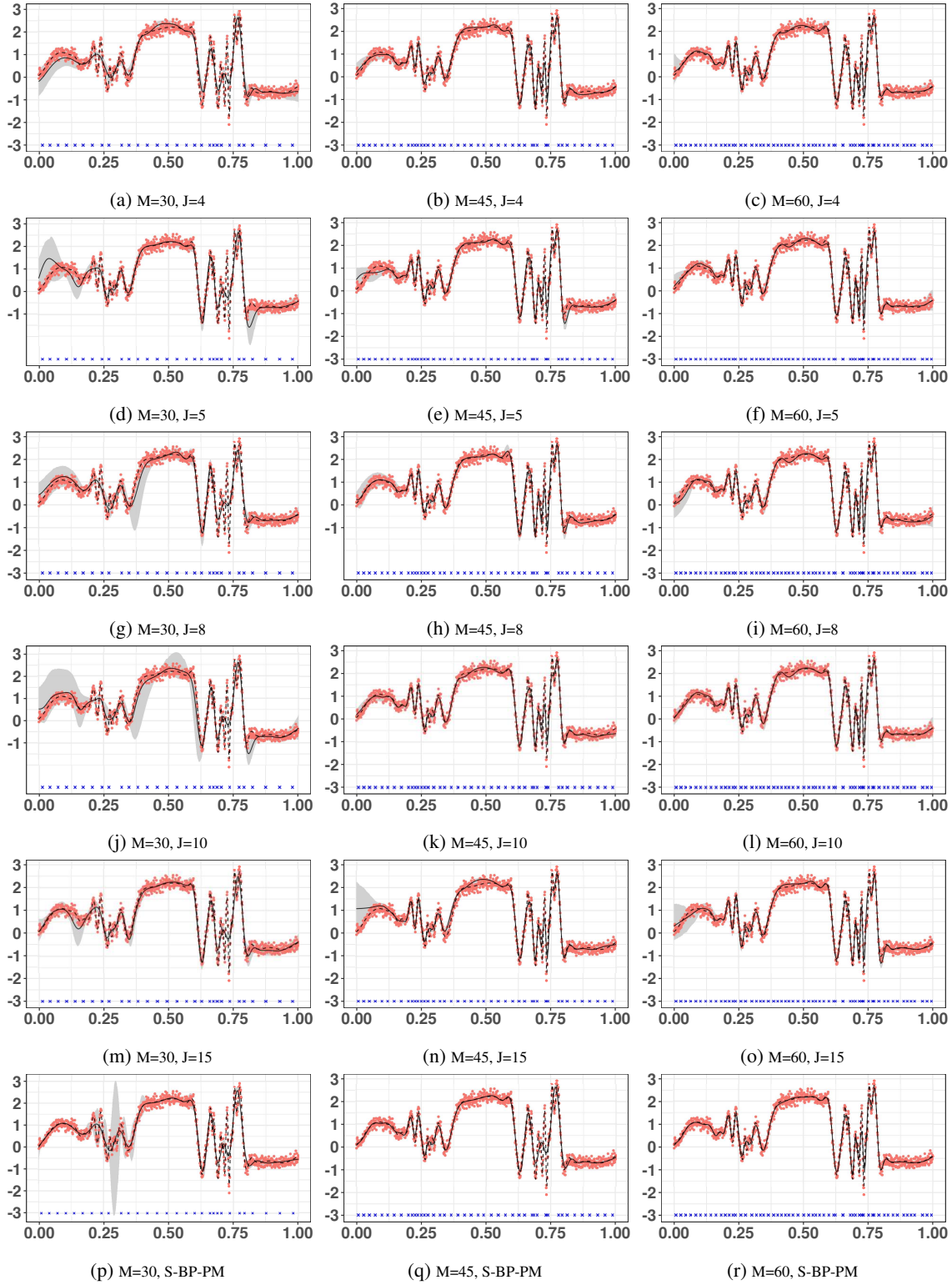


Figure 8: Predictions for different numbers of inducing points. The solid line denotes the predictive mean and the grey area depicts 95% HPD point-wise credible intervals. The dashed line denotes the true process.